



**Calhoun: The NPS Institutional Archive**  
**DSpace Repository**

---

Theses and Dissertations

Thesis and Dissertation Collection

---

1986-12

Diffraction radiation from relativistic electron bunches.

Gallet, Michael James

---

<http://hdl.handle.net/10945/21793>

*Downloaded from NPS Archive: Calhoun*



Calhoun is a project of the Dudley Knox Library at NPS, furthering the precepts and goals of open government and government transparency. All information contained herein has been approved for release by the NPS Public Affairs Officer.

**Dudley Knox Library / Naval Postgraduate School**  
**411 Dyer Road / 1 University Circle**  
**Monterey, California USA 93943**

<http://www.nps.edu/library>

# NAVAL POSTGRADUATE SCHOOL

Monterey, California



## THESIS

DIFFRACTION RADIATION FROM  
RELATIVISTIC ELECTRON BUNCHES

by

Michael James Gallet  
December 1986

Thesis Advisor:

Fred R. Buskirk

Approved for public release; distribution is unlimited

T230483

## REPORT DOCUMENTATION PAGE

1a REPORT SECURITY CLASSIFICATION UNCLASSIFIED			1b RESTRICTIVE MARKINGS		
2a SECURITY CLASSIFICATION AUTHORITY			3 DISTRIBUTION/AVAILABILITY OF REPORT Approved for public release; distribution is unlimited		
2b DECLASSIFICATION/DOWNGRADING SCHEDULE					
4 PERFORMING ORGANIZATION REPORT NUMBER(S)			5 MONITORING ORGANIZATION REPORT NUMBER(S)		
6a NAME OF PERFORMING ORGANIZATION Naval Postgraduate School		6b OFFICE SYMBOL (If applicable) Code 61	7a NAME OF MONITORING ORGANIZATION Naval Postgraduate School		
6c ADDRESS (City, State, and ZIP Code) Monterey, California 93943-5000			7b ADDRESS (City, State, and ZIP Code) Monterey, California 93943-5000		
8a NAME OF FUNDING/SPONSORING ORGANIZATION		8b OFFICE SYMBOL (If applicable)	9 PROCUREMENT INSTRUMENT IDENTIFICATION NUMBER		
8c ADDRESS (City, State, and ZIP Code)			10 SOURCE OF FUNDING NUMBERS		
			PROGRAM ELEMENT NO	PROJECT NO	TASK NO
			WORK UNIT ACCESSION NO		
11 TITLE (Include Security Classification) DIFFRACTION RADIATION FROM RELATIVISTIC ELECTRON BUNCHES					
12 PERSONAL AUTHOR(S) Gallet, Michael J.					
13a TYPE OF REPORT Master's Thesis		13b TIME COVERED FROM _____ TO _____		14 DATE OF REPORT (Year, Month, Day) 1986, December	
15 PAGE COUNT 65					
16 SUPPLEMENTARY NOTATION					
17 COSATI CODES			18 SUBJECT TERMS (Continue on reverse if necessary and identify by block number)		
FIELD	GROUP	SUB-GROUP			
			Diffraction Radiation;		
			Electron Diffraction Radiation		
19 ABSTRACT (Continue on reverse if necessary and identify by block number)					
<p>Diffraction radiation is that electromagnetic energy which is caused by a relativistic charged particle passing through an aperture in an opaque material. Ter-Mikaelian solved for the diffraction radiation from a point charge. This paper discusses the phenomena resulting from finite, relativistic charge bunches.</p> <p>Using the Huygens-Fresnel principle, diffraction patterns from spherical and cylindrical charge distributions are found and plotted. For charge bunch sizes less than the radiation wavelength, the results are almost identical to those for point charges.</p> <p>The radiation pattern is composed of two regions. The "transition region" is characterized by a strong peak at <math>\theta = \gamma^{-1}</math>, the Lorentz factor. The "diffraction region" consists of a series of peaks and nulls in field</p>					
20 DISTRIBUTION/AVAILABILITY OF ABSTRACT <input checked="" type="checkbox"/> UNCLASSIFIED/UNLIMITED <input type="checkbox"/> SAME AS RPT <input type="checkbox"/> DTIC USERS			21 ABSTRACT SECURITY CLASSIFICATION Unclassified		
22a NAME OF RESPONSIBLE INDIVIDUAL Prof. Fred R. Buskirk			22b TELEPHONE (Include Area Code) (408) 646-2765		22c OFFICE SYMBOL Code 61BS

UNCLASSIFIED

SECURITY CLASSIFICATION OF THIS PAGE (When Data Entered)

#19 - ABSTRACT - (CONTINUED)

strength typical of the standard plane wave  
diffraction pattern.

UNCLASSIFIED

SECURITY CLASSIFICATION OF THIS PAGE (When Data Entered)

Approved for public release; distribution is unlimited

Diffraction Radiation from  
Relativistic Electron Bunches

by

Michael James Gallet  
Lieutenant, United States Navy  
B.S., United States Naval Academy, 1981

Submitted in partial fulfillment of the  
requirements for the degree of

MASTER OF SCIENCE IN PHYSICS

from the

NAVAL POSTGRADUATE SCHOOL  
December 1986

## ABSTRACT

Diffraction radiation is that electromagnetic energy which is caused by a relativistic charged particle passing through an aperture in an opaque material. Ter-Mikaelian solved for the diffraction radiation from a point charge. This paper discusses the phenomena resulting from finite, relativistic charge bunches.

Using the Huygens-Fresnel principle, diffraction patterns from spherical and cylindrical charge distributions are found and plotted. For charge bunch sizes less than the radiation wavelength, the results are almost identical to those for point charges.

The radiation pattern is composed of two regions. The "transition region" is characterized by a strong peak at  $\theta = \gamma^{-1}$ , the Lorentz factor. The "diffraction region" consists of a series of peaks and nulls in field strength typical of the standard plane wave diffraction pattern.



## TABLE OF CONTENTS

I.	INTRODUCTION -----	7
A.	BACKGROUND -----	7
B.	THE VIRTUAL PHOTON -----	8
C.	DIFFRACTION THEORY BASED ON HUYGENS' PRINCIPLE -----	10
D.	FRESNEL AND FRAUNHOFER DIFFRACTION -----	12
II.	COMPUTATION OF DIFFRACTION RADIATION -----	16
A.	SOLUTION FOR A POINT CHARGE -----	16
B.	SOLUTION FOR A SPHERICAL CHARGE BUNCH -----	18
C.	DIFFRACTION RADIATION FROM A LARGE SPHERE OF CHARGE -----	25
D.	DIFFRACTION RADIATION FROM A CYLINDRICAL CHARGE BUNCH -----	31
E.	APPROXIMATIONS AND LIMITATIONS -----	38
III.	PARAMETERS AFFECTING DIFFRACTION RADIATION -----	39
A.	DEPENDENCE OF DIFFRACTION RADIATION ON $\gamma$ ----	40
B.	DEPENDENCE OF DIFFRACTION RADIATION ON BUNCH RADIUS -----	43
C.	DEPENDENCE OF DIFFRACTION RADIATION ON APERTURE RADIUS -----	45
IV.	DIFFRACTION RADIATION POWER -----	49
V.	CONCLUSIONS -----	51
APPENDIX A:	EVALUATION OF LINE CHARGE APPROXIMATION FOR CYLINDRICAL BUNCH -----	53
APPENDIX B:	DIFFERENCES WITH THE THEORY OF TER-MIKAELIAN -----	58
LIST OF REFERENCES	-----	61

BIBLIOGRAPHY -----	62
INITIAL DISTRIBUTION LIST -----	63



## I. INTRODUCTION

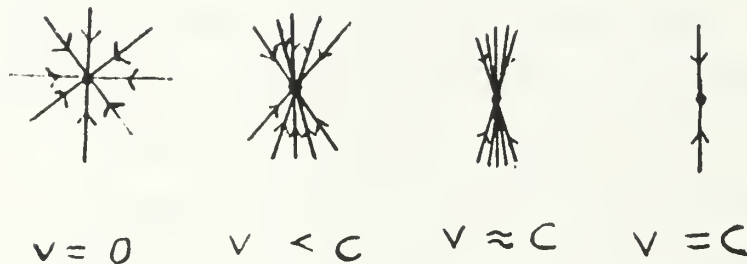
### A. BACKGROUND

Diffraction radiation occurs when a relativistic charged particle passes through a hole in a conductive or dielectric material. This phenomenon is very well understood for single, infinitesimal charges. Ter-Mikaelian computed the diffraction radiation for a single, relativistic electron. [Ref. 1] Less understood are the effects of charge bunching. Presumably, bunch sizes on the order of the radiation wavelength will significantly affect the diffraction radiation intensity by destructive interference. This paper discusses diffraction radiation from charge bunches with radii greater than zero but less than the radiation wavelength. Diffraction radiation will be computed for spherical and cylindrical bunch shapes. In addition, the effects of bunch size, beam energy, and aperture radius will be explored.

When electrons are travelling at relativistic velocities, they can be treated as "pseudo-photons." A method very similar to that used in physical optics based on the Huygens principle is then used to find the diffraction radiation pattern. [Ref. 1:p. 376] Panofsky and Phillips describe the "virtual photon concept" in Reference 2.

## B. THE VIRTUAL PHOTON

The electric field from a "fast electron" approaches that of a plane wave as the electron's velocity approaches  $c$ , the speed of light in a vacuum. Representations of the E-fields of electrons at various velocities are shown below:



For a uniformly moving electron, one can solve the Lienard-Wiechert potentials to find the field as viewed by a stationary observer. One finds the component of the electric field perpendicular to the electron's motion is very much greater than the parallel component and is given by

$$E_{\perp}(t) = \frac{1}{4\pi\epsilon_0} \gamma \frac{eb}{(b^2 + (vt\gamma)^2)^{3/2}}$$

where:

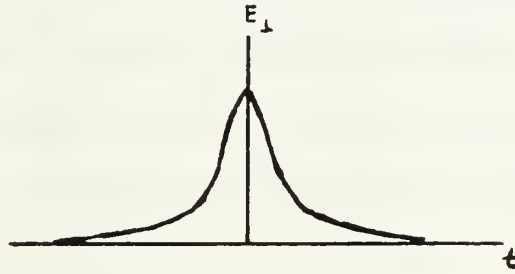
$e$  = the electron charge;

$b$  = the perpendicular distance from the electron's path;

$\gamma$  = the Lorentz factor =  $(\sqrt{1 - \beta^2})^{-1}$ ;

$\beta$  =  $v/c$ .

One can view this field as a sharp pulse of electromagnetic energy. The magnitude of this pulse is highly dependent on  $\gamma$ , which defines the relativistic energy of the electron. In addition, the duration of the pulse decreases as the electron energy rises. The electric field of an ultra-relativistic electron will appear very nearly as a delta function in the time domain. A representation of this electromagnetic pulse is shown below:



The Fourier transform of  $E_{\perp}(t)$  gives the frequency components of this pulse.

$$\begin{aligned}
 E_{\omega\perp} &= \frac{1}{2\pi} \int_{-\infty}^{\infty} E_{\perp}(t) e^{i\omega t} dt \\
 &= \frac{eb\gamma^{-2}}{8\pi^2 \epsilon_0} \int_{-\infty}^{\infty} \frac{e^{i\omega t}}{[(vt)^2 + \gamma^{-2}b^2]^{3/2}} dt \\
 &= \frac{e}{8\pi^2 \epsilon_0 bv} \int_{-\infty}^{\infty} \frac{e^{i(\frac{\omega b}{v\gamma})\xi}}{(\xi^2 + 1)^{3/2}} d\xi
 \end{aligned}$$

where:

$$\xi = \frac{\gamma vt}{b} .$$

Integrating, Panofsky and Phillips found

$$E_{\omega \perp} = \frac{e}{4\pi^2 \epsilon_0 b v} \left[ \left( \frac{\omega b}{v \gamma} \right) K_1 \left( \frac{\omega b}{v \gamma} \right) \right]$$

where  $K_1$  is the modified Bessel function of the second kind.  $K_1(x)$  approaches infinity as  $1/x$  near  $x = 0$  and goes to zero as  $e^{-x}$  for arguments greater than one. Panofsky and Phillips, as well as Ter-Mikaelian in his development of diffraction radiation, approximated  $E_{\omega \perp}$  by equating

$$E_{\omega \perp} = \begin{cases} \frac{e}{4\pi^2 \epsilon_0 b v} & \text{for } \omega < \frac{\gamma v}{b} \\ 0 & \text{for } \omega > \frac{\gamma v}{b} . \end{cases}$$

In his treatment of diffraction radiation from a single particle, Ter-Mikaelian assumes that the Fourier components of  $E_{\omega \perp}$  are spatially limited to a circle of radius  $b \approx \lambda \gamma$ . He states that the particle will radiate at a frequency  $\omega$  only when  $\lambda \gamma > r_0$ , where  $r_0$  is the characteristic dimension of the aperture. [Ref. 1:p. 377]

### C. DIFFRACTION THEORY BASED ON HUYGENS' PRINCIPLE

Ter-Mikaelian used Huygens' principle to compute the diffraction radiation pattern from a charged particle passing

through an opening. He thought of each point in the aperture as a source of secondary waves and then integrated over the aperture to find the total field at some distant observation point. The field at each point within the aperture is assumed to be unaffected by the obstruction. In practice, edge effects will be apparent for small apertures.

Huygens Principle states that:

every point on a primary wavefront serves as the source of spherical secondary wavelets such that the primary wavefront at some later time is in the envelope of these wavelets. Moreover, the wavelets advance with a speed and frequency equal to that of the primary wave at each point in space. [Ref. 3:pp. 60-61]

Using this theory, one can describe the propagation of a wave past an obstruction or aperture by mathematically summing the contributions of each "Huygens wavelet." Fresnel expanded upon Huygens' principle by stating:

every unobstructed point of a wavefront, at a given instant in time, serves as a source of spherical secondary wavelets (of the same frequency as the primary wave). The amplitude of the optical field at any point beyond is the superposition of all of these wavelets (considering their amplitudes and relative phases). [Ref. 3:p. 330]

There are some problems in using the Huygens-Fresnel principle, most notably the effects of electron oscillators at the edge of the aperture. Remember that Ter-Mikaelian assumed that the field within the aperture was unaffected by the obstruction. Oscillating electron "clouds" at the edge of the aperture will produce their own contributions to the total electric field within the aperture. The field is then made up of a part from the incident electric wave and one from

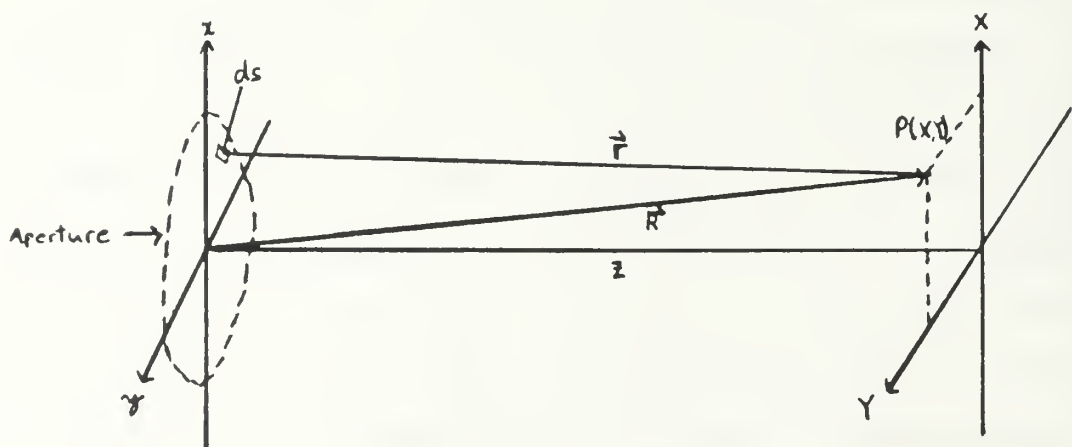
the induced oscillations at the edge of the obstruction. However, for apertures larger than the wavelength of the incident radiation, Huygens-Fresnel diffraction theory is expected to provide quite accurate results.

#### D. FRESNEL AND FRAUNHOFER DIFFRACTION

If the observation plane is located relatively far from the aperture, one can ignore the vector aspects of wave propagation and use the scalar Huygens-Fresnel principles. For each small source at the primary wavefront, the contribution to the field at observation point  $P(X,Y)$  is given by

$$dE_p(X,Y) = E_a(x,y) \exp i(\omega t - kr) ds/r$$

The exponential term provides the phase information and the  $r$  term in the denominator takes into account spherical spreading. A diagram of the problem is shown below:



In the typical diffraction problem encountered in the study of physical optics, a plane wave is assumed at the aperture, so the electric field across the aperture has no spatial variation in amplitude, polarization or phase. When dealing with the radiation from charged particles, however, one must consider that the field is radial with amplitude changing with distance from the charge. In our problem, we locate the observation point on the X-axis and deal only with the x-component of the field at the aperture. The field is symmetric about the Z-axis.

The total field at P(X,0) is given by the superposition of all the Huygens wavelets from all the sources at P(x,y) of size ds across the aperture.

$$E_{F,X}(X,0) = \int_{\text{Aperture}} E(x,y) \frac{\exp i(\omega t - kr)}{r} ds$$

This is a very difficult integral to evaluate in that the exponential term has a modulus of  $2\pi$ , making it difficult to make an asymptotic approximation.

The phase factor can be approximated by taking the binomial expansion of r and approximating it to the first order.

$$\begin{aligned} r^2 &= z^2 + (X-x)^2 + (0-y)^2 = z^2 + x^2 - 2Xx + x^2 + y^2 \\ &= (z^2 + x^2) - 2Xx + x^2 + y^2 \\ &= R^2(1 - 2Xx/R^2 + (x^2 + y^2)/R^2) \end{aligned}$$



where:

$$R^2 = X^2 + Z^2$$

so

$$r = R(1 - 2Xx/R^2 + (x^2 + y^2)/R^2)^{1/2} .$$

The binomial expansion is given by

$$(1 + x)^n = 1 + nx + \frac{n(n-1)}{2!} x^2 + \dots$$

To first order,

$$r = R - Xx/R + (x^2 + y^2)/2R .$$

The total field at P(X,0) becomes

$$E_{P,X}(X,0) = e^{i(\omega t - \kappa R)} \int_{\text{Aperture}} \frac{E_{a,x}(x,y)}{r} \\ \times e^{i\kappa((x^2+y^2)/2R - Xx/R)} ds .$$

For large R, one can replace the r in the denominator with R and the integral becomes

$$E_{P,X}(X,0) = \frac{e^{i(\omega t - \kappa R)}}{R} \int E_{a,x}(x,y) e^{-i\kappa(\frac{x^2+y^2}{2R} - \frac{Xx}{R})} ds .$$

If  $R$  is much greater than the aperture size and the phase difference from all of the incremental sources,  $ds$ , across the aperture is negligible, then the  $k(x^2+y^2)/2R$  term in the exponential is very small and may be neglected. In general, if this term is less than one radian, then the integral can be approximated by

$$E_{p,x}(X,0) = \frac{e^{i(\omega t - kR)}}{R} \int E_{a,x}(x,y) \exp(ikXx/R) ds .$$

In the Fraunhofer approximation the electric field at a distant point is just the two-dimensional Fourier transform of the electric field in the aperture.

## II. COMPUTATION OF DIFFRACTION RADIATION

### A. SOLUTION FOR A POINT CHARGE

A single relativistic electron has a Fourier spectrum, as derived earlier, given by

$$E_{\omega \perp} = \frac{e}{4\pi \epsilon_0 b v} \left[ \left( \frac{\omega b}{v\gamma} \right) K_1 \left( \frac{\omega b}{v\gamma} \right) \right] .$$

Using the Fraunhofer method, the field at a distant observation point is given by

$$E_{p,X}(X,0,Z) = \frac{e^{i(\omega t - \kappa R)}}{Z} \int_{\text{Aperture}} E_{a,X}(x,y) e^{ikXx/R} dS$$

where the x-component of the field at the aperture is given by

$$E_{a,X} = \frac{e}{4\pi \epsilon_0 b v} \left[ \left( \frac{\omega b}{v\gamma} \right) K_1 \left( \frac{\omega b}{v\gamma} \right) \right] \cos \theta .$$

Changing to polar coordinates gives us

$$\begin{aligned} & \frac{e^{i(\omega t - \kappa R)}}{Z} \int_0^{t_0} \int_0^{2\pi} \frac{e}{4\pi \epsilon_0 b v} \left[ \left( \frac{\omega b}{v\gamma} \right) K_1 \left( \frac{\omega b}{v\gamma} \right) \right] \cos \theta e^{ikXb \cos \theta / R} b d\theta db \\ &= \frac{e^{i(\omega t - \kappa R)}}{Z} \frac{e}{4\pi \epsilon_0 v} \int_0^{t_0} \left( \frac{\omega b}{v\gamma} \right) K_1 \left( \frac{\omega b}{v\gamma} \right) \int_0^{2\pi} \cos \theta e^{i(kbX/R) \cos \theta} d\theta db . \end{aligned}$$

Integrating over  $d\theta$  yields

$$\begin{aligned} & \frac{e^{i(\omega t - \kappa R)}}{Z} \frac{e}{4\pi\epsilon_0 v} 2\pi i \left(\frac{\omega}{v\gamma}\right) \int_0^{r_0} b K_1\left(\frac{\omega b}{v\gamma}\right) J_1\left(\frac{\kappa X}{R} b\right) db \\ &= \frac{e^{i(\omega t - \kappa R)}}{Z} \frac{ie}{2\pi\epsilon_0 v} \left(\frac{\omega}{v\gamma}\right) \left[ \frac{r_0}{\left(\frac{\kappa X}{R}\right)^2 + \left(\frac{\omega}{v\gamma}\right)^2} \left\{ \kappa \frac{X}{R} J_2\left(\kappa r_0 \frac{X}{R}\right) K_1\left(\frac{\omega r_0}{v\gamma}\right) \right. \right. \\ & \quad \left. \left. - \frac{\omega}{v\gamma} J_1\left(\kappa r_0 \frac{X}{R}\right) K_2\left(\frac{\omega r_0}{v\gamma}\right) \right\} \right] \end{aligned}$$

which contains the final form of the diffraction radiation pattern. As Ter-Mikaelian did in Reference 1, the radiation field is found by subtracting the particle field from the results above. The particle field is found by letting  $r_0$  go to infinity in the integral over the aperture. It is interesting to note that as  $r_0$  goes to infinity, the diffraction radiation field strength goes to zero. Physically, at this point the electron no longer "feels" the presence of the obstruction.

Ter-Mikaelian, in Reference 1, computes the diffraction radiation from a charged particle passing through a circular aperture. Using the method outlined in the previous section, he determines (for  $\alpha r_0 \ll 1$ )

$$E_{p,X}(X,0) = \frac{ie}{2\pi\epsilon c} \frac{q}{q^2 + \alpha^2} J_0(q r_0) ,$$

where:

$$\alpha = \frac{\omega}{v\gamma} ;$$

$$q = k \sin \theta = \frac{\text{the projection of the wave vector } \vec{k} \text{ on the plane } z = 0;}{k}$$

$$r_0 = \text{the aperture radius.}$$

This result appears to be significantly different from the expression derived earlier. In reality, however, the two plots are virtually identical. (See Appendix B.)

#### B. SOLUTION FOR A SPHERICAL CHARGE BUNCH

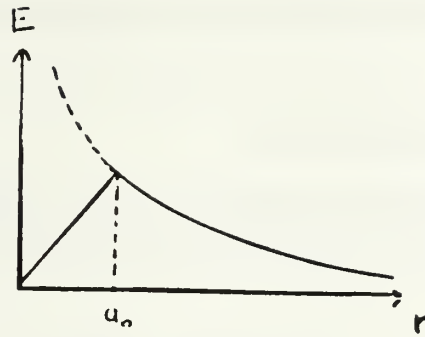
The diffraction problem has been solved for single charged particle radiation.

The process for a finite charge bunch can be solved, as a first approximation, by assuming a spherical charge distribution of radius  $a_0$  with constant charge density,  $\rho$ .

In the frame of the moving charge, the electric field is radial with a magnitude given by

$$E = \begin{cases} \frac{1}{3\epsilon_0} r \rho & \text{for } r \leq a_0 \\ \frac{a_0^3 \rho}{3\epsilon_0 r^2} & \text{for } r \geq a_0 \end{cases}$$

This result is easily obtained using Gauss' law. A representation of  $E(r)$  is shown below.



To find the field from the moving charge distribution in the frame of a stationary observer, one must find the Lorentz transformation of the radial field. With a spherical charge distribution, an observer views a field emanating from the center of the charge bunch; the field from the uniform spherical distribution appears to be a point charge equal to the total charge of the sphere. If the observer is located within the sphere, he still "sees" a point source, but of a reduced strength (that portion of the sphere's charge enclosed by a Gaussian surface). Consequently, the Lorentz transformation of the moving spherical charge bunch must have a form similar to that of the point charge. In the lab frame, one finds a perpendicular electric field of

$$E_{\perp}(t) = \begin{cases} \frac{4/3 \pi a_o^3 \rho}{4\pi\epsilon_o} \frac{\gamma^{-2} b}{[(vt)^2 + \gamma^{-2} b^2]^{3/2}} & \text{for } b \geq a_o \\ \frac{4/3 \pi b^3 \rho}{4\pi\epsilon_o} \frac{\gamma^{-2} b}{[(vt)^2 + \gamma^{-2} b^2]^{3/2}} & \text{for } b \leq a_o \end{cases}$$

This form of  $E(t)$  is only approximate for  $b < a_0$ . For small bunches ( $a_0 \ll \tau_0$ ), the error introduced by this approximation is negligible.

Since  $E(t)$  of the sphere has the same time dependence as that of the point charge, it must have Fourier components of the same form.

$$E_{\perp\omega} = \begin{cases} \frac{4/3\pi a_0^3 \rho}{4\pi^2 \epsilon_0 b v} \left[ \left( \frac{\omega b}{v\gamma} \right) K_1 \left( \frac{\omega b}{v\gamma} \right) \right] & \text{for } b \geq a_0 \\ \frac{4/3\pi b^3 \rho}{4\pi^2 \epsilon_0 b v} \left[ \left( \frac{\omega b}{v\gamma} \right) K_1 \left( \frac{\omega b}{v\gamma} \right) \right] & \text{for } b \leq a_0 \end{cases}$$

Again,  $E_{\omega\perp}$  is negligible for  $\lambda < b/\gamma$ , we make the additional requirement that the wavelength be large compared to the bunch size in order that the bunch radiate coherently.

Again, one proceeds using the Huygens-Fresnel principle to find the radiation pattern from the spherical bunch passing through a circular aperture. With the observation point located on the X-axis, one expects to see only an X-component to the perpendicular field. Due to symmetry, only the x-component of the field across the aperture contributes to the total field at  $P(X,0)$ . The transverse electric field at  $P(X,0)$  is given by

$$E_{p,X}(X,0,Z) = \frac{e^{i(\omega t - kR)}}{Z} \int_{\text{Aperture}} E_{a,X}(x,y) e^{ikXx/R} ds$$



where the x-component of the field at the aperture is given by

$$E_{a,X} = \begin{cases} \frac{4/3\pi a_o^3 \rho}{4\pi^2 \epsilon_o b v} \left[ \left( \frac{\omega b}{v\gamma} \right) K_1 \left( \frac{\omega b}{v\gamma} \right) \right] \cos \theta & \text{for } b \leq a_o \\ \frac{4/3\pi b^3 \rho}{4\pi^2 \epsilon_o b v} \left[ \left( \frac{\omega b}{v\gamma} \right) K_1 \left( \frac{\omega b}{v\gamma} \right) \right] \cos \theta & \text{for } b > a_o \end{cases}$$

Changing to polar coordinates yields

$$E_{p,X} = \frac{e^{i(\omega t - \kappa R)}}{Z} \int E_{a,X}(b, \theta) e^{i(kXb \cos \theta/R)} ds$$

where:

$$ds = b d\theta db$$

Finally, one obtains

$$\begin{aligned} & \frac{e^{i(\omega t - \kappa R)}}{Z} \int E_{a,X}(b, \theta) e^{i(kXb \cos \theta/R)} b d\theta db \\ &= \frac{e^{i(\omega t - \kappa R)}}{Z} \left[ \int_0^{a_o} \int_0^{2\pi} \frac{4/3\pi b^3 \rho}{4\pi^2 \epsilon_o b v} \left[ \left( \frac{\omega b}{v\gamma} \right) K_1 \left( \frac{\omega b}{v\gamma} \right) \right] \cos \theta e^{i(kXb \cos \theta/R)} b d\theta db \right. \\ & \quad \left. + \int_{a_o}^{\infty} \int_0^{2\pi} \frac{4/3\pi a_o^3 \rho}{4\pi^2 \epsilon_o b v} \left[ \left( \frac{\omega b}{v\gamma} \right) K_1 \left( \frac{\omega b}{v\gamma} \right) \right] \cos \theta e^{i(kXb \cos \theta/R)} b d\theta db \right] \end{aligned}$$

We shall first solve for the integral from  $b = 0$  to  $a_0$ ;  
we have

$$\int_0^{a_0} \int_0^{2\pi} \frac{4/3\pi b^3 \rho}{4\pi^2 \epsilon_0 v} \left[ \left( \frac{\omega b}{v\gamma} \right) K_1 \left( \frac{\omega b}{v\gamma} \right) \right] \cos \theta e^{i(kXb \cos \theta/R)} b d\theta db$$

$$= \frac{4/3\pi \rho}{4\pi^2 \epsilon_0 v} \int_0^{a_0} b^3 \left( \frac{\omega b}{v\gamma} \right) K_1 \left( \frac{\omega b}{v\gamma} \right) \int_0^{2\pi} \cos \theta e^{i(kXb \cos \theta/R)} d\theta db .$$

The integral over  $d\theta$  is equal to  $(2\pi i)J_1(kXb/R)$ . The integral becomes

$$2\pi i \frac{4/3\pi \rho}{4\pi^2 \epsilon_0 v} \int_0^{a_0} b^3 \left( \frac{\omega b}{v\gamma} \right) K_1 \left( \frac{\omega b}{v\gamma} \right) J_1 \left( \frac{kXb}{R} \right) db .$$

As an example, one can expect to see parameters in an experiment on diffraction radiation in the micro-wave region as follows:

$$f = 8 \text{ GHz}$$

$$a_0 = 0.5 \text{ cm}$$

$$\gamma_{\min} = 20$$

$$v \approx c = 3 \times 10^{10} \text{ cm/s}$$

$$k = 2\pi/\lambda = 1.675 \text{ cm}^{-1}$$

$$X/R = \sin \theta \text{ where } \theta \text{ is the angle between } \vec{k} \text{ and the } Z\text{-axis.}$$

Using these values, the maximum values of the arguments in  $K_1(x)$  and  $J_1(x)$  in the integral from 0 to  $a_0$  are

$$(\omega b / \gamma v) = 8.33 \times 10^{-2}$$

$$(kXb/R) = 8.38 \times 10^{-1}$$

With these values for arguments, the two Bessel functions in the integral can be very closely approximated by

$$K_1(x) = 1/x$$

and

$$J_1(x) = x/2 .$$

The integral becomes

$$2\pi i \frac{4/3\pi\rho}{4\pi\epsilon_0 v} \int_0^{a_0} b^3 \frac{1}{2} \left(\frac{kXb}{R}\right) db = 2\pi i \frac{4/3\pi\rho}{4\pi^2\epsilon_0 v} \left(\frac{1}{2} K\right) \left(\frac{a_0}{5}\right)^5 \sin \theta .$$

We next evaluate the integral from  $a_0$  to  $r_0$ . Since the integral here has the same  $\theta$ -dependence as in the previous case, the integral becomes

$$2\pi i \frac{4/3\pi a_0^3 \rho}{4\pi^2\epsilon_0 v} \int_{a_0}^{r_0} \left(\frac{\omega b}{\gamma v}\right) K_1\left(\frac{\omega b}{\gamma v}\right) J_1\left(\frac{kXb}{R}\right) db .$$

Note that in this case, we have not made the approximations for the two Bessel functions since  $b$  will in practice extend to values much larger than one wavelength. This integral can be easily solved and yields

$$\begin{aligned}
\int_0^{r_0} \left(\frac{\omega b}{v\gamma}\right) K_1\left(\frac{\omega b}{v\gamma}\right) J_1\left(\frac{kXb}{R}\right) db &= \left(\frac{1}{\left(\frac{kX}{R}\right)^2 + \left(\frac{\omega}{v\gamma}\right)^2}\right) \\
&\times \left[ r_0 \left\{ \left(\frac{kX}{R}\right) K_1\left(\frac{\omega r_0}{v\gamma}\right) J_2\left(\frac{kXr_0}{R}\right) - \frac{\omega}{v\gamma} J_1\left(\frac{kXr_0}{R}\right) K_2\left(\frac{\omega r_0}{v\gamma}\right) \right. \right. \\
&\left. \left. - a_0 \left\{ \left(\frac{kX}{R}\right) K_1\left(\frac{\omega a_0}{v\gamma}\right) J_2\left(\frac{kXa_0}{R}\right) - \frac{\omega}{v\gamma} J_1\left(\frac{kXa_0}{R}\right) K_2\left(\frac{\omega a_0}{v\gamma}\right) \right\} \right\} \right]
\end{aligned}$$

Combining the solutions of the two integrals and subtracting the particle field, the total transverse field at  $P(X,0)$  is given by

$$\begin{aligned}
E_{P,X}(X,0) &= \frac{e^{i(\omega t - kR)}}{Z} (2\pi i) \frac{4/3\pi a_0^3}{4\pi \epsilon v} \left\{ \left\{ \frac{1}{2} \left(\frac{kX}{R}\right) \left(\frac{a_0^2}{5}\right) + \frac{\omega}{v\gamma} \left(\frac{1}{\left(\frac{kX}{R}\right)^2 + \left(\frac{\omega}{v\gamma}\right)^2}\right) \right. \right. \\
&\left. \left[ r_0 \left\{ \left(\frac{kX}{R}\right) K_1\left(\frac{\omega r_0}{v\gamma}\right) J_2\left(\frac{kXr_0}{R}\right) - \frac{\omega}{v\gamma} J_1\left(\frac{kXr_0}{R}\right) K_2\left(\frac{\omega r_0}{v\gamma}\right) \right\} \right. \right. \\
&\left. \left. - a_0 \left\{ \left(\frac{kX}{R}\right) K_1\left(\frac{\omega a_0}{v\gamma}\right) J_2\left(\frac{kXa_0}{R}\right) - \frac{\omega}{v\gamma} J_1\left(\frac{kXa_0}{R}\right) K_2\left(\frac{\omega a_0}{v\gamma}\right) \right\} \right\} \right\} \\
&\left. - \frac{k \sin \theta}{(k \sin \theta)^2 + \left(\frac{\omega}{v\gamma}\right)^2} \right\}
\end{aligned}$$

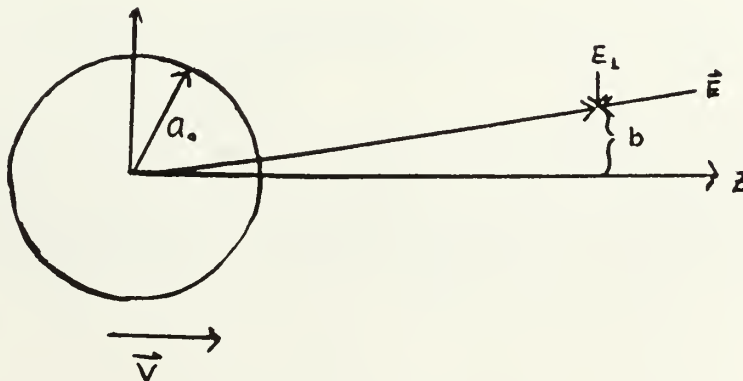
### C. DIFFRACTION RADIATION FROM A LARGE SPHERE OF CHARGE

For diffraction problems where the radiation contribution from within the charge bunch is significant (i.e.,  $a_0 \sim r_0$ ), one can not make the approximation used in the previous section where  $E_{\perp}$  had the same time dependence for  $b < a_0$  as it did for  $b > a_0$ . In this section, we shall gain a more exact understanding of the problem by determining the diffraction radiation from a large sphere of charge.

Using Gauss's law, one finds

$$E_r = \begin{cases} \frac{\rho}{4\pi\epsilon} \frac{4/3\pi a_0^3}{r^2} \frac{b}{r} & \text{for } r \geq a_0 \\ \frac{\rho}{4\pi\epsilon} \frac{4/3\pi r^3}{r^2} \frac{b}{r} & \text{for } r \leq a_0 \end{cases}$$

where  $b/r$  provides the perpendicular component of  $\vec{E}$ , as shown below:



This relation reduces to

$$E_r = \frac{\rho}{4\pi\epsilon} \begin{cases} \frac{4/3\pi a_o^3 b}{r^3} & \text{for } r > a_o \\ 4/3 \pi b & \text{for } r < a_o . \end{cases}$$

A representation for  $E_{\perp}$  is shown below for several values of  $b$ :

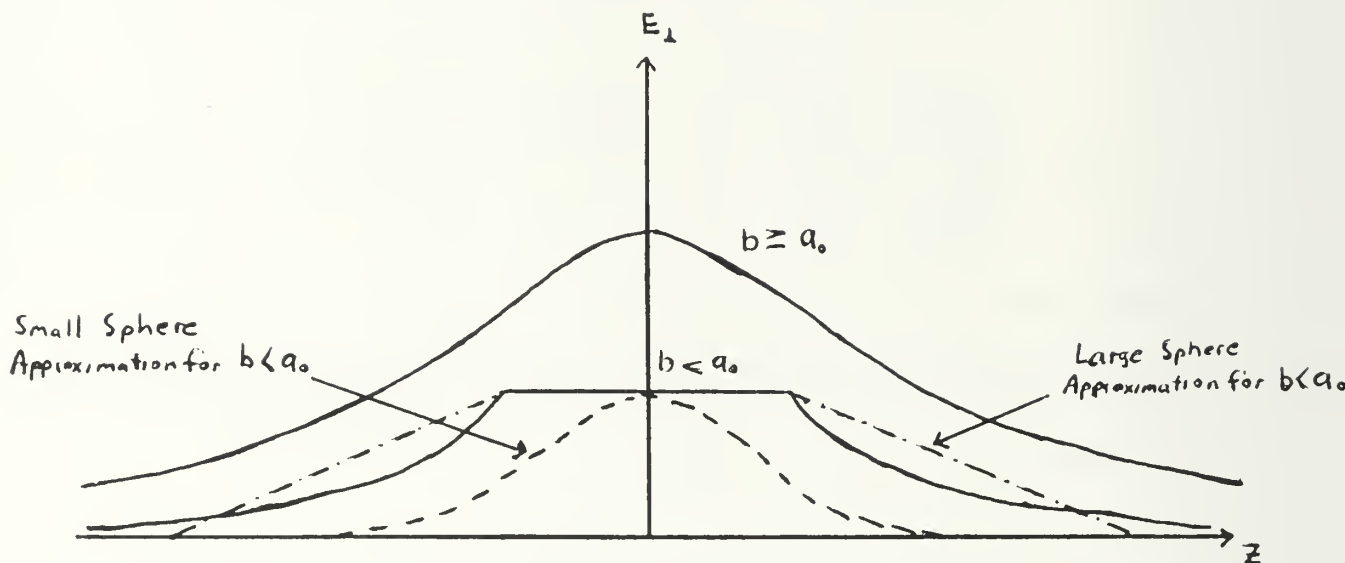


Figure 1

This function for  $b < a_o$  can be integrated numerically only. However, one can make a very close approximation for  $E$  with  $b < a_o$  by writing

$$E_{\perp} = \frac{\rho}{4\pi\epsilon} \begin{cases} \frac{4/3\pi b(1.5a_o - z)}{1.5a_o - \sqrt{a_o^2 - b^2}} & \text{for } \sqrt{a_o^2 - b^2} < z < 1.5a_o \\ 4/3\pi b & \text{for } -\sqrt{a_o^2 - b^2} < z < \sqrt{a_o^2 - b^2} \\ \frac{4/3\pi b(1.5a_o + z)}{1.5a_o - \sqrt{a_o^2 - b^2}} & \text{for } -1.5a_o < z < -\sqrt{a_o^2 - b^2} \end{cases}$$

This approximation is shown on Figure 1. For most values of  $b$ , this linear approximation to the  $1/r^3$  dependence of  $E_{\perp}(r)$  outside the sphere lies very close to the actual curve. This is particularly true as  $b$  approaches  $a_o$ , where most of the diffraction radiation from within the sphere is expected to originate. Replacing  $z$  with  $-vt$ ,  $E(t)$  is equal to

$$E_{\perp}(t) = \frac{\rho}{4\pi\epsilon} \begin{cases} \frac{4/3\pi a_o^2 b}{(b^2 + (vt)^2)^{3/2}} & \text{for } b > a_o \\ \frac{4/3\pi b(1.5a_o + vt)}{1.5a_o - \sqrt{a_o^2 - b^2}} & \text{for } b < a_o, \sqrt{a_o^2 - b^2} < -vt < 1.5a_o \\ 4/3\pi b & \text{for } b < a_o, -\sqrt{a_o^2 - b^2} < -vt < \sqrt{a_o^2 - b^2} \\ \frac{4/3\pi b(1.5a_o - vt)}{1.5a_o - \sqrt{a_o^2 - b^2}} & \text{for } b < a_o, -1.5a_o < -vt < -\sqrt{a_o^2 - b^2} \end{cases}$$

For a relativistic electron bunch, the Lorentz transformation gives



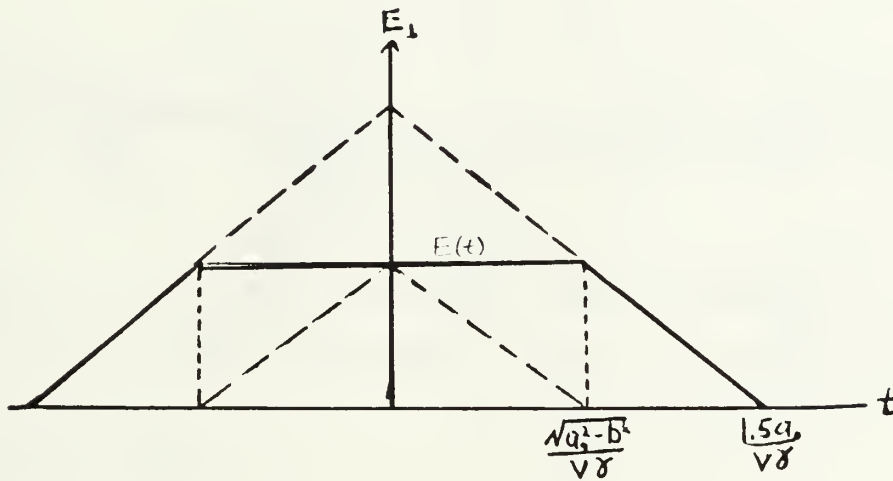
$$E(t) = \frac{\rho}{4\pi\epsilon} \gamma \left\{ \begin{array}{ll} \frac{4/3\pi a_o^3 b}{(b^2 + (\gamma vt)^2)^{3/2}} & \text{for } b > a_o \\ \frac{4/3\pi b(1.5a_o + \gamma vt)}{1.5a_o - \sqrt{a_o^2 - b^2}} & \text{for } b < a_o, -\frac{\sqrt{a_o^2 - b^2}}{\gamma} < -vt < \frac{1.5a_o}{\gamma} \\ 4/3\pi b & \text{for } b < a_o, \frac{-\sqrt{a_o^2 - b^2}}{\gamma} < -vt < \frac{\sqrt{a_o^2 - b^2}}{\gamma} \\ \frac{4/3\pi b(1.5a_o - \gamma vt)}{1.5a_o - \sqrt{a_o^2 - b^2}} & \text{for } b < a_o, \frac{-1.5a_o}{\gamma} < -vt < \frac{-\sqrt{a_o^2 - b^2}}{\gamma} \end{array} \right.$$

or

$$E(t) = \frac{\rho}{4\pi\epsilon} \gamma \left\{ \begin{array}{ll} \frac{4/3\pi a_o^3 b}{(b^2 + (\gamma vt)^2)^{3/2}} & \text{for } b > a_o \\ \frac{4/3\pi b(1.5a_o + \gamma vt)}{1.5a_o - \sqrt{a_o^2 - b^2}} & \text{for } b < a_o, \frac{-1.5a_o}{v\gamma} < t < \frac{-\sqrt{a_o^2 - b^2}}{v\gamma} \\ 4/3\pi b & \text{for } b < a_o, |t| < \frac{\sqrt{a_o^2 - b^2}}{v\gamma} \\ \frac{4/3\pi b(1.5a_o - \gamma vt)}{1.5a_o - \sqrt{a_o^2 - b^2}} & \text{for } b < a_o, \frac{\sqrt{a_o^2 - b^2}}{v\gamma} < t < \frac{1.5a_o}{v\gamma} \end{array} \right.$$

The diffraction radiation found by integrating over the aperture from  $a_o$  to  $r_o$  for the large sphere of charge will be identical to that found in the small sphere approximation and need not be discussed here.

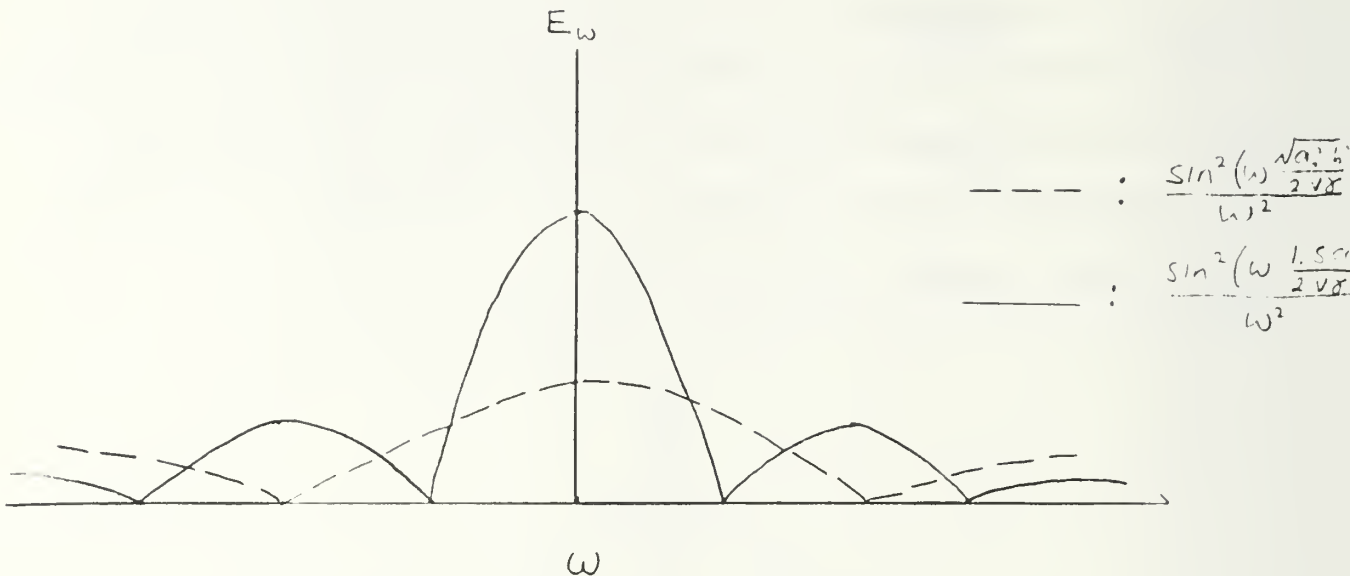
This section will discuss only that radiation originating from the aperture for  $0 < b < a_0$ . For this range of  $b$ , the Fourier components of the field are found by writing  $E_{\perp}(t)$  as a difference of two simple functions whose Fourier transforms are tabulated in any introductory text on Fourier analysis.  $E_{\perp}(t)$  is written as the difference of two triangular pulses, as shown below:



It is easily seen that

$$E_{\omega\perp} = \frac{\rho\gamma}{4\pi\epsilon} \left\{ 4 \left( \frac{4/3\pi b(1.5a_0)}{1.5a_0 - \sqrt{a_0^2 - b^2}} \right) \frac{\sin^2(\omega \frac{1.5a_0}{2v\gamma})}{\omega^2} \right. \\ \left. - 4 \left( \frac{4/3\pi b(1.5a_0)}{1.5a_0 - \sqrt{a_0^2 - b^2}} \right) - 4/3\pi b \right) \frac{\sin^2(\omega \frac{\sqrt{a_0^2 - b^2}}{2v\gamma})}{\omega^2} \right\}.$$

A diagram of a typical contribution to  $E_{\omega}$  from each function is shown below:



One can easily see that  $E_{\omega_{\perp}}$  is cut off at high frequencies.

The field at a distant observation site  $P(X,0,Z)$  is given in the usual manner by

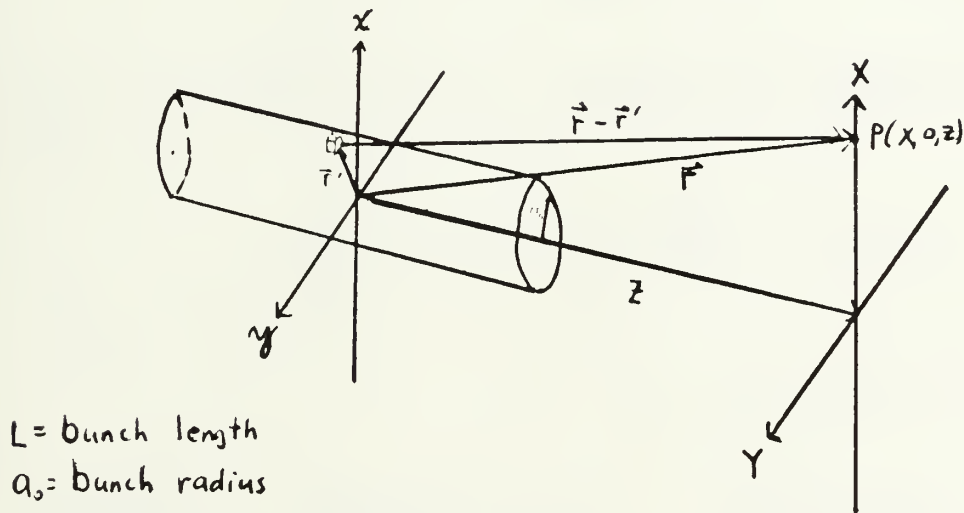
$$\begin{aligned}
 E_{P,X}(X,0,Z) &= \frac{e^{i(\omega t - \kappa R)}}{Z} \int_0^{a_0} \int_0^{2\pi} E_{\omega_{\perp}} \cos \theta e^{i(kXb \cos \theta/R)} b db d\theta \\
 &= \frac{e^{i(\omega t - \kappa R)}}{Z} 2\pi i \int_0^{a_0} E_{\omega_{\perp}} J_1\left(\frac{kXb}{R}\right) b db .
 \end{aligned}$$

This integral can be evaluated numerically to find the diffraction radiation pattern from a large sphere of charge. When this is done, the results are not accurate enough to make detailed predictions regarding the diffraction pattern.

They do show, however, that the diffraction pattern from a large sphere of charge is consistent with that found for small bunches. The field strengths are significantly less, but the pattern of peaks and nulls is roughly the same.

#### D. DIFFRACTION RADIATION FROM A CYLINDRICAL CHARGE BUNCH

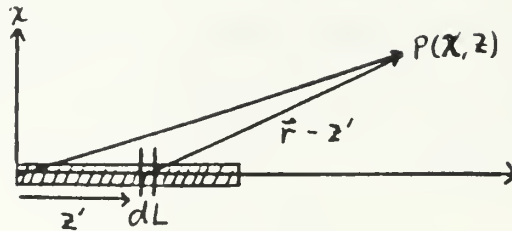
Consider first a stationary charge distribution with axes as shown below:



We wish to find the electric field at an observation point  $P(X, Y)$ . By cylindrical symmetry, the electric field at an observation point on the  $X$ -axis will have only  $\hat{i}$  and  $\hat{k}$  components. We are interested primarily in the  $\hat{i}$  component since, for the relativistic electron bunch,  $E_{\perp} \gg E_{\parallel}$ .

In order to solve for  $E_{\perp}$ , one must first find the electrostatic solution for a cylindrical bunch. One can make an approximation by treating the cylindrical bunch as a line

charge of linear charge density  $\rho(\pi a_o^2)$ . For  $b < a_o$ , the linear charge density is given by  $\rho(\pi b^2)$ . A diagram of the problem is shown below:



For  $b > a_o$

$$E(X, Z) = \frac{\rho \pi a_o^2}{4\pi\epsilon} \int \frac{x}{(X^2 + (Z-z')^2)^{3/2}} dz'$$

Let  $u = Z-z$ ;  $du = dz$ .

$$\begin{aligned} E_{\perp} &= \frac{\rho \pi a_o^2}{4\pi\epsilon} \int_{Z-L}^Z \frac{b}{(b^2 + u^2)^{3/2}} du = \frac{\rho \pi a_o^2}{4\pi\epsilon} b \left[ \frac{1}{b^2} \frac{u}{(b^2 + u^2)^{1/2}} \right]_{Z-L}^Z \\ &= \frac{\rho \pi a_o^2}{4\pi\epsilon} \frac{1}{b} \left( \frac{Z}{(b^2 + Z^2)^{1/2}} - \frac{Z-L}{(b^2 + (Z-L)^2)^{1/2}} \right) \end{aligned}$$

For a slow moving bunch, located at the aperture at  $t = 0$ , one can substitute  $(-vt)$  for  $Z$  and write the time varying field at the aperture as

$$E_{\perp}(t) = \frac{\rho \pi a_o^2}{4\pi\epsilon b} \left( \frac{(-vt)}{(b^2 + (vt)^2)^{1/2}} + \frac{vt+L}{(b^2 + (vt+L)^2)^{1/2}} \right) .$$

For a relativistic charge bunch, the component of the electric field perpendicular to the bunch path is given by

$$E(t) = \begin{cases} \frac{\rho \pi b^2}{4\pi \epsilon b} \gamma \left( \frac{-vt\gamma}{(b^2 + (vt\gamma)^2)^{1/2}} + \frac{(vt\gamma + L)}{(b^2 + (vt\gamma + L)^2)^{1/2}} \right) & \text{for } b < a_0 \\ \frac{\rho \pi a_0^2}{4\pi \epsilon b} \gamma \left( \frac{-vt\gamma}{(b^2 + (vt\gamma)^2)^{1/2}} + \frac{(vt\gamma + L)}{(b^2 + (vt\gamma + L)^2)^{1/2}} \right) & \text{for } b > a_0 \end{cases}$$

As in the previous section, the Fourier components of the field for  $b > a_0$  are given by

$$\begin{aligned} E_{\omega \perp} &= \frac{1}{2\pi} \int_{-\infty}^{\infty} E_{\perp}(t) e^{i\omega t} dt \\ &= \frac{1}{2\pi} \frac{\rho \pi a_0^2}{4\pi \epsilon b} \gamma \left\{ \int_{-\infty}^{\infty} \frac{(vt\gamma + L) e^{i\omega t}}{(b^2 + (vt\gamma + L)^2)^{1/2}} dt - \int_{-\infty}^{\infty} \frac{vt\gamma e^{i\omega t}}{(b^2 + (vt\gamma)^2)^{1/2}} dt \right\} \end{aligned}$$

Evaluating the first integral, one finds

$$\int_{-\infty}^{\infty} \frac{(vt\gamma + L) e^{i\omega t}}{\sqrt{b^2 + (vt\gamma + L)^2}} dt = \int_{-\infty}^{\infty} \frac{(\frac{vt\gamma + L}{b}) e^{i\omega t}}{\sqrt{1 + (\frac{vt\gamma + L}{b})^2}} dt$$

letting  $\psi = (vt\gamma + L)/b$ ;  $t = (b\psi/v\gamma) - (L/v\gamma)$ ; and  $d\psi = (v\gamma/b)dt$ , the integral becomes

$$\frac{b}{v\gamma} \int_{-\infty}^{\infty} \frac{\psi e^{i\omega(\frac{b}{v\gamma}\psi - \frac{L}{v\gamma})}}{\sqrt{1+\psi^2}} d\psi = \frac{b}{v\gamma} e^{\frac{i\omega L}{v\gamma}} \int_{-\infty}^{\infty} \frac{\psi e^{\frac{i\omega b}{v\gamma}\psi}}{\sqrt{1+\psi^2}} d\psi.$$

Using the equation  $e^{i\theta} = \cos \theta + i \sin \theta$  and remembering the properties of even and odd Fourier integrals, the integral is rewritten as

$$i \frac{2b}{v\gamma} e^{\frac{i\omega L}{v\gamma}} \int_0^{\infty} \frac{\psi \sin(\frac{\omega b}{v\gamma}\psi)}{\sqrt{1+\psi^2}} d\psi = i \frac{2b}{v\gamma} e^{\frac{i\omega L}{v\gamma}} K_1\left(\frac{\omega b}{v\gamma}\right).$$

Using the same techniques to evaluate the second integral in  $E_{\omega 1}$ , one finds

$$E_{\omega 1} = \begin{cases} \frac{i}{2\pi} \frac{\rho \pi a_o^2}{4\pi \epsilon b} \gamma \left(\frac{2b}{v\gamma}\right) K_1\left(\frac{\omega b}{v\gamma}\right) (e^{\frac{i\omega L}{v\gamma}} - 1) & \text{for } b \geq a_o \\ \frac{i}{2\pi} \frac{\rho \pi b^2}{4\pi \epsilon b} \gamma \left(\frac{2b}{v\gamma}\right) K_1\left(\frac{\omega b}{v\gamma}\right) (e^{\frac{i\omega L}{v\gamma}} - 1) & \text{for } b \leq a_o. \end{cases}$$

As previously explained, the Hankel transform of the field at the circular aperture is evaluated to find the field at observation point  $P(X,0)$ .



$$E_{p,X} = \frac{e^{i(\omega t - \kappa R)}}{Z} \frac{i}{2\pi} \left[ \int_0^{a_0} \int_0^{2\pi} \frac{\rho \pi b^2}{4\pi \epsilon b} \gamma \left( \frac{2b}{v_Y} \right) K_1 \left( \frac{\omega b}{v_Y} \right) (e^{\frac{i\omega L}{v_Y} - 1}) \cos \theta e^{ikXb \cos \theta / R} b db d\theta \right. \\ \left. + \int_{a_0}^{r_0} \int_0^{2\pi} \frac{\rho \pi a_0^2}{4\pi \epsilon b} \gamma \left( \frac{2b}{v_Y} \right) K_1 \left( \frac{\omega b}{v_Y} \right) (e^{\frac{i\omega L}{v_Y} - 1}) \cos \theta e^{ikXb \cos \theta / R} b db d\theta \right]$$

Simplifying, the equation becomes

$$E_{p,X} = \frac{e^{i(\omega t - \kappa R)}}{Z} \left( \frac{i}{2\pi} \frac{\rho \pi}{4\pi \epsilon} \gamma \left( \frac{2}{v_Y} \right) (e^{\frac{i\omega L}{v_Y} - 1}) \right) \\ \times \left[ \int_0^{a_0} \int_0^{2\pi} b^3 K_1 \left( \frac{\omega b}{v_Y} \right) e^{ikXb \cos \theta / R} \cos \theta db d\theta \right. \\ \left. + \frac{a_0^2}{a_0} \int_{a_0}^{r_0} \int_0^{2\pi} b K_1 \left( \frac{\omega b}{v_Y} \right) e^{ikXb \cos \theta / R} \cos \theta db d\theta \right].$$

As in the problem for a spherical charge bunch, integrating over  $d\theta$  gives

$$E_p(X, 0) = \frac{e^{i(\omega t - \kappa R)}}{Z} \left( - \frac{\rho \pi \gamma}{4\pi \epsilon} \left( \frac{2}{v_Y} \right) (e^{\frac{i\omega L}{v_Y} - 1}) \right) \\ \times \left[ \int_0^{a_0} b^3 K_1 \left( \frac{\omega b}{v_Y} \right) J_1 \left( \frac{kXb}{R} \right) db + \frac{a_0^2}{a_0} \int_{a_0}^{r_0} b K_1 \left( \frac{\omega b}{v_Y} \right) J_1 \left( \frac{kXb}{R} \right) db \right].$$

Evaluating the integral from 0 to  $a_0$ , one makes the usual approximation

$$\int_0^{a_0} b^3 K_1\left(\frac{\omega b}{v\gamma}\right) J_1\left(\frac{kXb}{R}\right) db \approx \frac{v\gamma}{\omega} \int b^2 J_1\left(\frac{kXb}{R}\right) db ,$$

since in this range,  $K_1(x) \sim 1/x$ . One finds

$$\frac{v\gamma}{\omega} \int_0^{a_0} b^2 J_1\left(\frac{kXb}{R}\right) db = \frac{v\gamma}{\omega} \left(\frac{R}{kX}\right) a_0^2 J_2\left(\frac{kXa_0}{R}\right) .$$

Next, evaluate the integral from  $a_0$  to  $r_0$ .

$$\begin{aligned} a_0^2 \int_{a_0}^{r_0} b K_1\left(\frac{\omega b}{v\gamma}\right) J_1\left(\frac{kXb}{R}\right) db &= a_0^2 \frac{1}{\left(\frac{kX}{R}\right)^2 + \left(\frac{\omega}{v\gamma}\right)^2} \\ &\times \left( r_0 \left\{ \frac{kX}{R} J_2\left(\frac{kXr_0}{R}\right) K_1\left(\frac{\omega r_0}{v\gamma}\right) - \frac{\omega}{v\gamma} J_1\left(\frac{kXr_0}{R}\right) K_2\left(\frac{\omega r_0}{v\gamma}\right) \right\} \right. \\ &\left. - a_0 \left\{ \frac{kX}{R} J_2\left(\frac{kXa_0}{R}\right) K_1\left(\frac{\omega a_0}{v\gamma}\right) - \frac{\omega}{v\gamma} J_1\left(\frac{kXa_0}{R}\right) K_2\left(\frac{\omega a_0}{v\gamma}\right) \right\} \right) . \end{aligned}$$

Since  $X/R = \sin \theta$ , the total field at the observation plane is

$$\begin{aligned}
E_p(X,0) &= \frac{e^{i(\omega t - \kappa R)}}{Z} \frac{\rho \pi a_o^2}{2\pi \epsilon v} (e^{i\frac{\omega L}{v\gamma}} - 1) \\
&\times \left\{ \left[ \frac{v\gamma}{\omega} \frac{1}{k \sin \theta} J_2(k \sin \theta a_o) \right. \right. \\
&+ \left. \left. \frac{1}{(k \sin \theta)^2 + (\frac{\omega}{v\gamma})^2} \right. \right. \\
&\quad \left. \left( \kappa_o \{ k \sin \theta J_2(k \sin \theta \kappa_o) K_1(\frac{\omega \kappa_o}{v\gamma}) - \frac{\omega}{v\gamma} J_1(k \sin \theta \kappa_o) K_2(\frac{\omega \kappa_o}{v\gamma}) \} \right. \right. \\
&\quad \left. \left. - a_o \{ k \sin \theta J_2(k \sin \theta a_o) K_1(\frac{\omega a_o}{v\gamma}) - \frac{\omega}{v\gamma} J_1(k \sin \theta a_o) K_2(\frac{\omega a_o}{v\gamma}) \} \right) \right\} \\
&\quad \left. - \frac{k \sin \theta}{(k \sin \theta)^2 + (\frac{\omega}{v\gamma})^2} \right\}
\end{aligned}$$

The effect of bunch length is in the  $(e^{i\frac{\omega L}{v\gamma}} - 1)$  term. Expanding the exponential in this term gives an imaginary and real part of the solution.

$$\begin{aligned}
(e^{i\frac{\omega L}{v\gamma}} - 1) &= e^{i(\frac{\omega L}{v\gamma})/2} 2i \frac{e^{i(\frac{\omega L}{v\gamma})/2} - e^{-i(\frac{\omega L}{v\gamma})/2}}{2i} \\
&= 2ie^{i(\frac{\omega L}{v\gamma})/2} \sin(\frac{\omega L}{2v\gamma})
\end{aligned}$$

At first glance, this function seems to give the diffraction an oscillating dependence on radiation frequency for all frequencies. One must remember, however, that the  $K_1(\omega a_0/v\gamma)$  term in the solution very nearly cuts off the radiation at  $\omega > v\gamma/a_0$ . The real and imaginary terms in this expression give an additional phase factor to the overall solution for diffraction radiation. For wavelengths much larger than bunch size, the real term is approximately zero and the dependence on bunch length is given by  $i(\frac{\omega L}{v\gamma})$ .

#### E. APPROXIMATIONS AND LIMITATIONS

The reader is cautioned to remember that in making the Fraunhofer approximation to the diffraction problem, one assumes:

- 1) The diffraction angle is small ( $< 1$  rad).
- 2) The phase difference from all "sources,"  $ds$ , across the aperture is small ( $k(x^2 + y^2)/2R < 1$ ).
- 3) The aperture size is greater than the wavelength of the incident radiation. (Neglect edge effects.)
- 4) Since charge was assumed to be uniformly distributed throughout the bunch, the quantized nature of charge was ignored. This can be done if the electron density is sufficiently high ( $n^{-1/3} < \lambda$ ).
- 5) Charge bunch sizes are assumed to be less than the radiation wavelength to ensure coherent radiation of the bunch. Larger bunches have smaller intensities due to destructive interference.

### III. PARAMETERS AFFECTING DIFFRACTION RADIATION

In the previous chapter, diffraction radiation was computed and, for a given frequency, was found to be dependent upon several parameters, namely  $\gamma$ , bunch radius,  $a_0$ , and aperture radius,  $r_0$ . In addition to these effects, the radiation is significantly cut-off at high frequencies.

Remembering that both the small sphere and cylindrical charge bunches had Fourier components proportional to  $(\omega b/v\gamma) K(\omega b/v\gamma)$ , one can make the approximation that the fields are small for  $\omega > v\gamma/b$ . (When the argument of  $K_1(x)$  is 1,  $xK(x) = .6019$ . This gives a field intensity of about one third the maximum value.) If the maximum value of  $b$  is the bunch radius,  $a_0$ , then the maximum value of  $\omega$  is given by  $\omega_{\max} = v\gamma/a_0$ . One expects radiation at  $2\omega_{\max}$  to be 10 dB less than the peak values.

Figure 2 can be used as a rough guide to the frequency dependence of observed radiation.

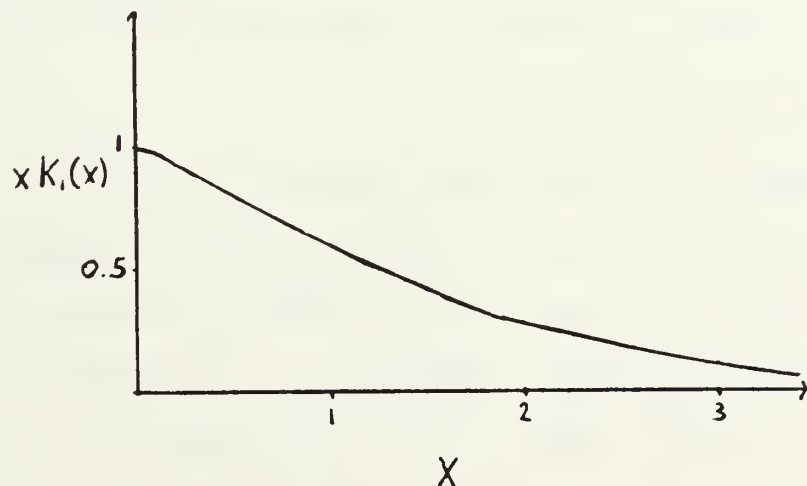


Figure 2

For the large sphere, the Fourier components of the fields were found to drop off as

$$\frac{\sin^2(.75 \frac{\omega a_0}{v\gamma})}{\omega^2}$$

One can say that the field is cut-off at  $\omega = v\gamma/a_0$ .

It is easily seen that, for each bunch shape discussed, the diffraction radiation is very near the peak values at microwave frequencies. A previous experiment at the NPS Linac discovered diffraction radiation in the microwave region ( $f = 8$  GHz) from a circular aperture [Ref. 4]. For  $f = 8$  GHz,  $\omega b/v\gamma K_1(\omega b/v\gamma)$  is very nearly equal to unity.

The plots of diffraction radiation vs.  $\theta$ , the off-axis angle, consist of two distinct regions. The first is characterized by a strong peak at  $\theta = \gamma^{-1}$ . Since the peak at  $\theta = \gamma^{-1}$  is typical of transition radiation, this region of the curve is called the "transition region."

At  $\theta \gg \gamma^{-1}$ , the radiation pattern appears more as the typical diffraction pattern of peaks and nulls. This region is called the "diffraction region."

#### A. DEPENDENCE OF DIFFRACTION RADIATION ON $\gamma$

The  $\gamma$ -dependent portion of the function describing diffraction radiation tends to be very complicated and hard to understand analytically. The strongest dependence is in the transition region, where a very strong peak in field strength occurs at  $\theta = \gamma^{-1}$ . In this region, the field strength is

very nearly given by  $(k \sin \theta) / ((k \sin \theta)^2 + (\omega/v\gamma)^2)$ . The strength of this peak is directly proportional to  $\gamma$ . In the diffraction region, the effect is less pronounced. One expects to see more diffraction radiation energy from electrons of higher energy. Figure 4 shows the dependence of diffraction radiation on  $\gamma$ . The curves for a cylindrical bunch will be identical to this figure. Increasing  $\gamma$  tends to sharpen the diffraction pattern, increasing the strength of the peaks in field strength.

For pseudo-photons of a given frequency, the transverse fields tend to extend farther out for increasing  $\gamma$ . Alternatively, the field for a given frequency and radial distance,  $b$ , tends to be higher for an increasing  $\gamma$ . Figure 3 demonstrates this point. If one compares the same Fourier components of two relativistic electrons with different energies, the more energetic electron's fields extend much further out than those of the less energetic electron.

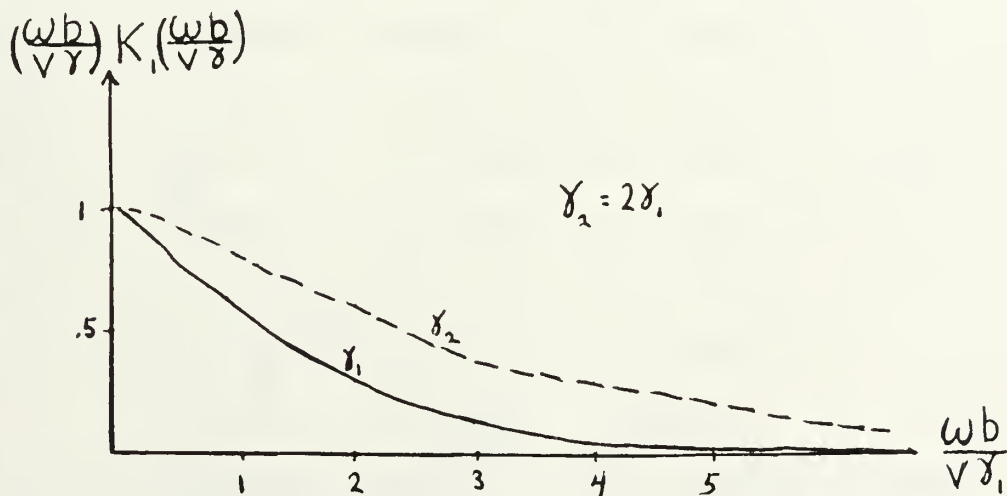


Figure 3

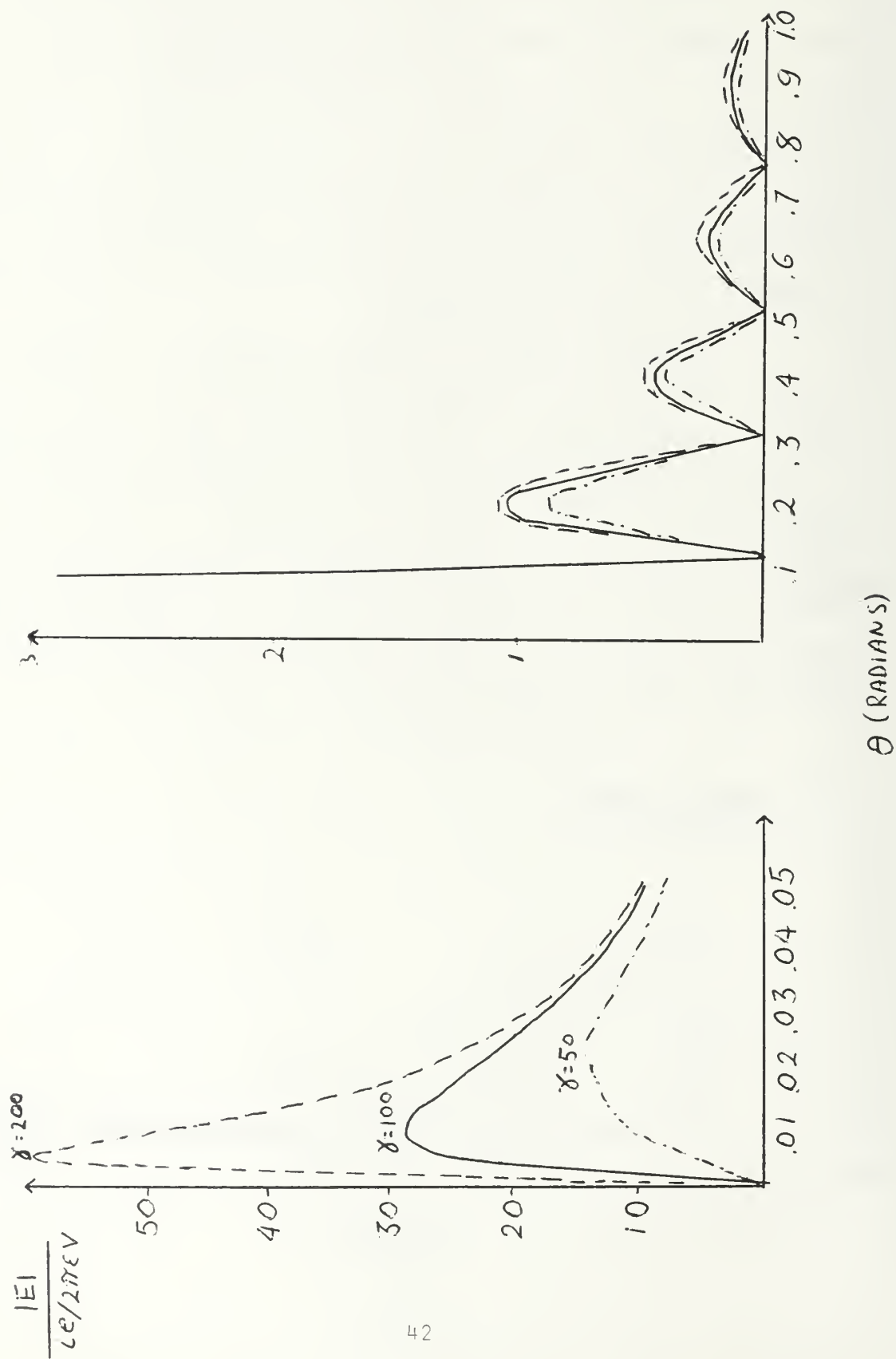


Figure 4:  $E$  vs  $\theta$  for various energies  $\chi$ .  $\chi=200$  (solid line),  $\chi=100$  (dashed line),  $\chi=50$  (dash-dot line).  $\theta$  is in radians.



Ter-Mikaelian determined that, for a point particle with  $\omega r_0/v\gamma \ll 1$ , the  $\gamma$ -dependence was given by

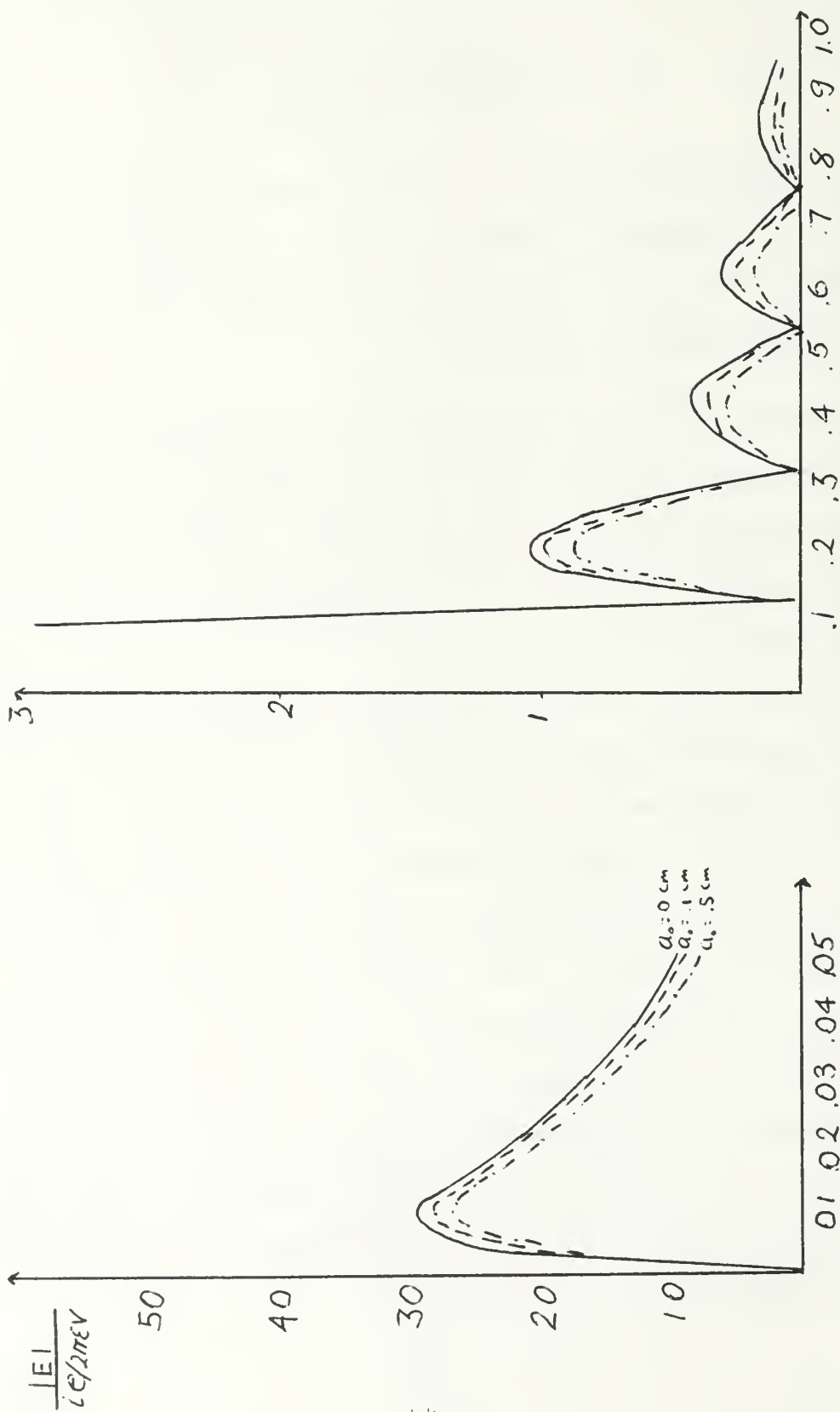
$$E \sim \frac{k \sin \theta}{(k \sin \theta)^2 + \left(\frac{\omega}{v\gamma}\right)^2}$$

The  $\gamma$ -dependence found in the last chapter for both cylindrical and spherical charge bunches is consistent with that of Ter-Mikaelian. One expects the fields to go to zero for non-relativistic particles.

#### B. DEPENDENCE OF DIFFRACTION RADIATION ON BUNCH RADIUS

Throughout this paper, we have assumed that the bunch radius is smaller than the wavelength of the radiation. When this is the case, one may assume coherent radiation from the bunch.

By examining the equations for diffraction radiation for all three bunch types, one can see that diffraction radiation tends to decrease for bunches with larger radii. For small bunch radii, a general decrease in the field strengths from the peak levels for infinitesimal bunch sizes is observed, as shown in Figure 5. For cylindrical bunches of equal charge, the diffraction radiation field strength is inversely proportional to  $L$ , where  $L$  is the bunch length. This is expected since the radial fields at the aperture are proportional to the charge/length within the bunch. The  $(e^{\omega L/v\gamma} - 1)$  factor also specifies a length at which coherent radiation from the bunch can be expected.



$\theta$  (RADIAN)

Figure 5: E vs  $\theta$  for various bunch radii  
 $\gamma = 100$ ,  $R = 10$  cm,  $f = 8$  GHz

One can easily understand the effect of bunch size by examining the static radial fields from a sphere of charge. The effect from a cylindrical charge bunch will be similar.

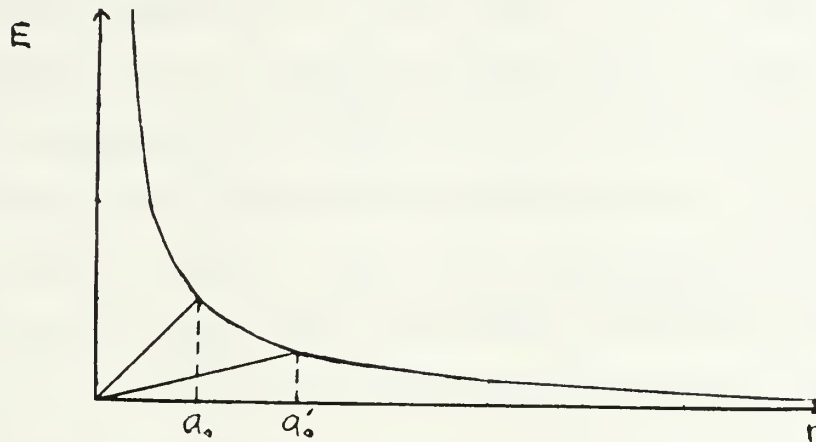


Figure 6

Figure 6 compares the fields from two spheres of radii  $a_0$  and  $a'_0$ . As shown earlier, for an infinitesimal sphere, the fields increase asymptotically to infinity as  $r$  goes to zero. For a sphere of radius  $a_0$ , the field increases with the same  $1/r$  dependence as  $r$  decreases from infinity to  $a_0$  and then drops off linearly to 0 at  $r = 0$ . One can easily see from the figure that the sphere of smaller radius is the source of more electrostatic energy than the larger sphere. As the sphere gets smaller, the total electrostatic energy rapidly approaches that of a point charge.

#### C. DEPENDENCE OF DIFFRACTION RADIATION ON APERTURE RADIUS

A plane wave incident upon a circular aperture results in the familiar Airy diffraction pattern. The large central maximum in intensity is known as the Airy disk. The

diffraction radiation pattern from a relativistic electron beam is very similar, except that the central maximum is replaced by a null. This central null results from the radial nature of the electron fields. In the Fraunhofer diffraction method, integrating over the aperture for  $d\theta$  results in a 0th order Bessel function of the first kind for the plane wave and a 1st order Bessel function for the electron diffraction radiation, thus explaining the principal difference in the two radiation patterns.

Figure 7 shows the diffraction radiation pattern for cylindrical and small spherical charge bunches passing through circular apertures of various radii. Changing the aperture size affects the diffraction radiation pattern in both the transition and diffraction regions. One can define a dimensionless parameter,  $kr_0$ , where  $\vec{k} = \frac{\omega}{c}\hat{k}$  = the wave vector and  $r_0$  is the aperture radius. This parameter alone determines the location of the peaks in the diffraction region. When  $kr_0$  increases, the peaks gain in strength and move in closer to the  $\theta = 0$  axis. Decreasing  $kr_0$  spreads the diffraction pattern out over wider angles. This is predicted since the diffraction radiation pattern is caused principally by the  $J_{1,2}(kr_0 \sin \theta)$  terms in the solution. Note that patterns with a large number of maxima and minima are found only for aperture sizes much larger than the wavelength of the observed radiation. This is to be expected since, for the normal diffraction of a plane wave, a small aperture acts

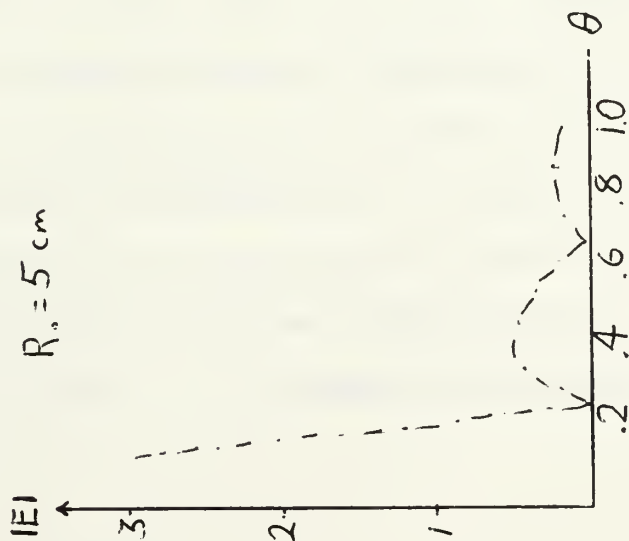
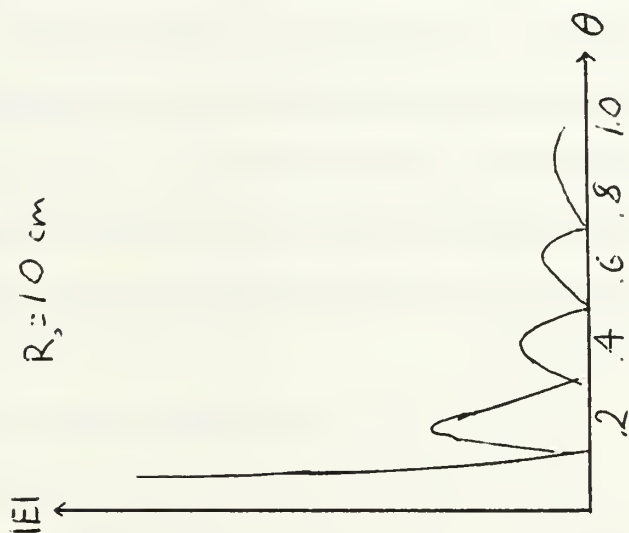
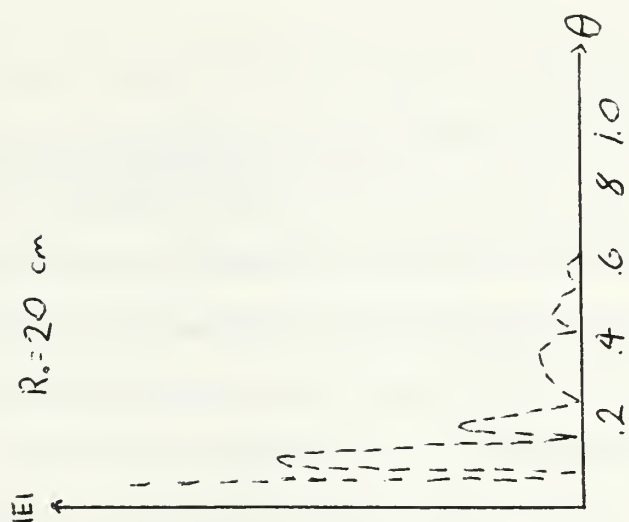
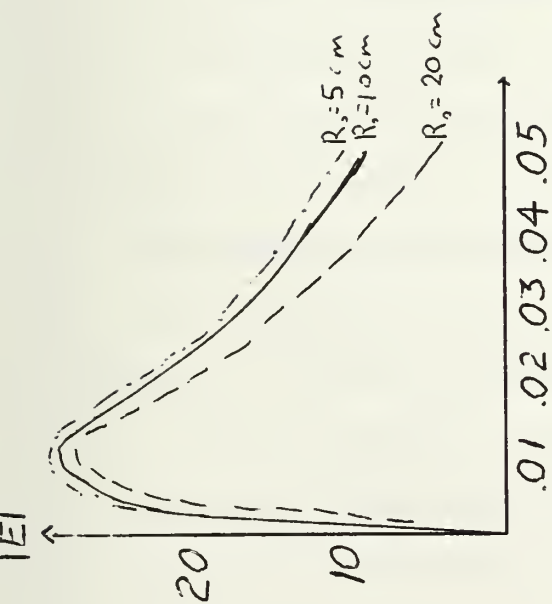


Figure 7:  $E$  vs  $\theta$  for various aperture radii  
 $a_s = .1 \text{ cm}$ ,  $f = 100$ ,  $f = 8 \text{ GHz}$

almost as an isotropic point source of radiation. In the case of diffraction radiation, we still see the null at  $\theta = 0$  due to the radial nature of the fields. Since the dimensionless parameter is given by  $k\tau_0$ , one can change the appearance of the diffraction pattern by changing  $\tau_0$ , the physical size of the aperture, or  $k$ , which determines the wavelength of the radiation.

In the transition region, changing the parameter,  $k\tau_0$ , affects the strength of the peak at  $\theta = \gamma^{-1}$ . As  $k\tau_0$  goes to zero the peak at  $\gamma^{-1}$  increases, asymptotically approaching the value characteristic of transition radiation. As  $k\tau_0$  increases, the strength of this peak decreases, until, as  $k\tau_0$  goes to infinity, the peak goes to zero. At this point, the charge no longer senses the obstruction and no energy is radiated.

One should also notice that the diffraction radiation pattern for spherical and cylindrical charge bunches are identical for bunch lengths less than the radiation wavelength. For very large charge bunches, interference effects are expected to reduce the overall intensity of radiation/ (bunch charge), but the location of maxima and minima will not change. The locations of the radiation pattern's maxima and minima are principally a function of radiation wavelength and aperture size, as it is in the normal plane wave diffraction problem.

#### IV. DIFFRACTION RADIATION POWER

It has been suggested that diffraction radiation may be used for electron beam targetting or in a non-interceptive beam diagnostic device. [Ref. 5]

Present diagnostic systems are based on the beam passing through a thin foil and using transition or Cerenkov radiation to analyze beam characteristics. The problem with this scheme is that the beam is disturbed by the foil. If the beam passes through an aperture, one can, in theory, obtain the same diagnostic information without disturbing the beam. If diffraction radiation is to be used as a diagnostic or targetting means, one must gain an appreciation for the power levels expected from a typical device.

For an electromagnetic wave given by

$$\vec{E} = \vec{E}_0 e^{i(\omega t - \kappa R)} ,$$

the power per unit area, or irradiance, is given by

$$I \equiv \langle S \rangle \equiv \frac{c E_0^2}{2} .$$

One can compute the diffraction radiation irradiance by using this expression together with the equations derived in Chapter II.



As an example, the diffraction radiation power delivered by a 1000 amp, 50 MeV electron beam passing through a 20 cm diameter circular aperture will be maximized at  $\theta = 10^\circ$ . If one assumes 10 cm long cylindrical bunches of radius .1 cm and evaluates the expression for diffraction radiation from a cylindrical charge bunch, the irradiance at  $Z = 1$  m from the aperture is equal to

$$I = \frac{CE_o}{2} E_o^2 = 500 \text{ KW/m}^2 .$$

The power per unit solid angle is 500 KW/SR.



## V. CONCLUSIONS

In this paper, the equations regarding diffraction radiation from a relativistic charge distribution passing through an aperture have been derived from the Huygens-Fraunhofer treatment of the fields across the aperture. The calculations are very similar to the familiar problem of plane wave diffraction solved in every physical optics class, with the complications that the fields are radial with varying field strength in space.

While a plane wave incident on a circular aperture causes a diffraction pattern with a large, central peak known as the Airy disk, the diffraction radiation pattern produced by electrons is characterized by a null at  $\theta = 0$  and is highly dependent upon aperture size. In addition, a strong peak at  $\theta = \gamma^{-1}$  is present, characteristic of transition radiation. If the aperture size is very small, the structure in the diffraction region disappears and the radiation pattern approaches that of pure transition radiation. The only radiation present is the strong peak at  $\theta = \gamma^{-1}$ . Increasing the aperture size, or more properly, the dimensionless parameter  $kr_0$ , decreases the peak at  $\theta = \gamma^{-1}$  and compresses the structure in the diffraction region. Eventually, as  $kr_0$  approaches infinity, the radiation goes to zero. The diffraction radiation pattern in the diffraction region exhibits

some dependence on electron energy but not nearly as strong as in the transition region. The radiation intensity in both the transition and diffraction regions has a minor dependence on bunch size.

Ter-Mikaelian describes diffraction radiation as having a strong peak at  $\theta = \gamma^{-1}$  followed by a broad series of peaks and nulls dependent on  $J_0(k \sin \theta r_0)$ . The diffraction patterns developed in this paper are primarily dependent on  $J_1(k \sin \theta r_0)$  and  $J_2(k \sin \theta r_0)$ , but when plotted are found to be in complete agreement with Ter-Mikaelian's results. Both results are in agreement on several key aspects of diffraction radiation:

- 1) There is a strong dependence of diffraction radiation on aperture size.
- 2) The diffraction radiation energy goes to zero as aperture size goes to infinity.
- 3) The diffraction radiation energy is dependent on the energy of the beam, described by  $\gamma$ .
- 4) The diffraction radiation exhibits a strong peak at  $\theta = \gamma^{-1}$ .

## APPENDIX A

### EVALUATION OF LINE CHARGE APPROXIMATION FOR CYLINDRICAL BUNCH

As described in Chapter II, the static fields for a cylindrical charge distribution were approximated by a modified line charge. The linear charge distribution was given by

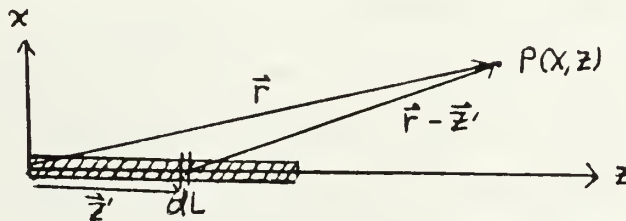
$$\lambda = \rho \pi a_0^2 \text{ C/cm} ,$$

where:

$a_0$  = cylindrical bunch radius in cm

$\rho$  = charge density of cylindrical charge bunch in  $\text{C/cm}^3$ .

When  $b$ , the off-axis distance, is less than  $a_0$  the linear charge density was given by  $\lambda = \rho \pi b^2$ .



For the geometry shown above, the field for the line charge is given by

$$\frac{\rho \pi a_o^2}{4\pi\epsilon} \frac{1}{b} \left( \frac{z}{(b^2 + z^2)^{1/2}} - \frac{z-L}{(b^2 + (z-L)^2)^{1/2}} \right) .$$

As a check of this approximation, the fields predicted by the linear approximation were compared to the fields resulting from the actual cylinder of charge, which were computed by numerically integrating

$$\frac{\rho}{4\pi\epsilon} \int_{r=0}^{a_o} \int_{\theta=0}^{2\pi} \int_{z=0}^L \frac{X - r \cos \theta}{((X-r \cos \theta)^2 + (r \sin \theta)^2 + (Z-Z')^2)^{3/2}} r dr d\theta dz .$$

Figure A.1.1 shows the comparison for three "long" cylinders ( $L \gg a_o$ ), where the observation point is outside of the cylinder ( $b > a_o$ ). The linear approximation is expected to work best in this situation.

As can be seen from the figure, the approximation is very close for the cylinders of lengths 1 cm and 2 cm and is identical for the longer 10 cm bunch. The radial fields become very nearly equal to that of an infinitely long line of charge very close to the ends of the bunch.

The linear approximation is expected to perform worst for a relatively short, thick cylinder of charge when the observation point is on the interior of the cylinder.

Figure A1.2 shows the comparison for these cylinders ranging in relative length from  $L = a_o$  to  $L \gg a_o$ . For the shorter length, the approximate fields are found to rise slightly more sharply and to higher levels than the actual

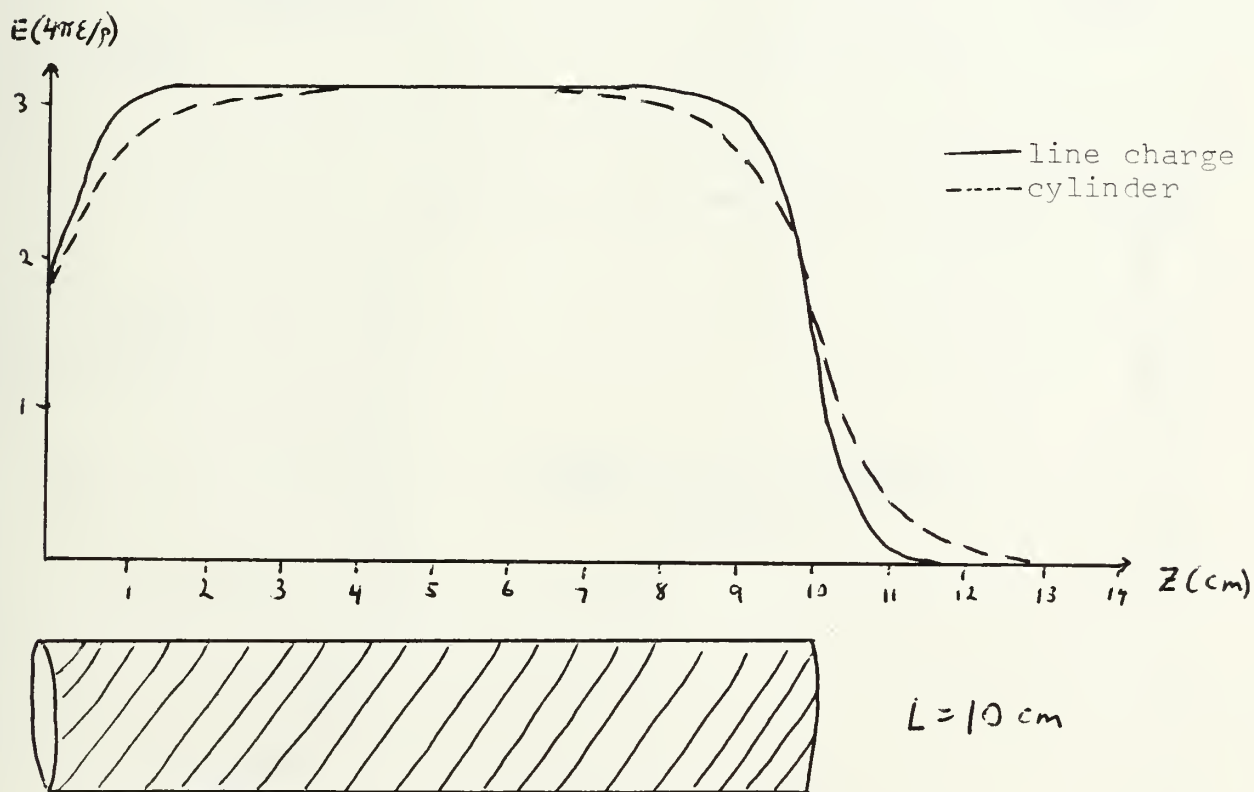
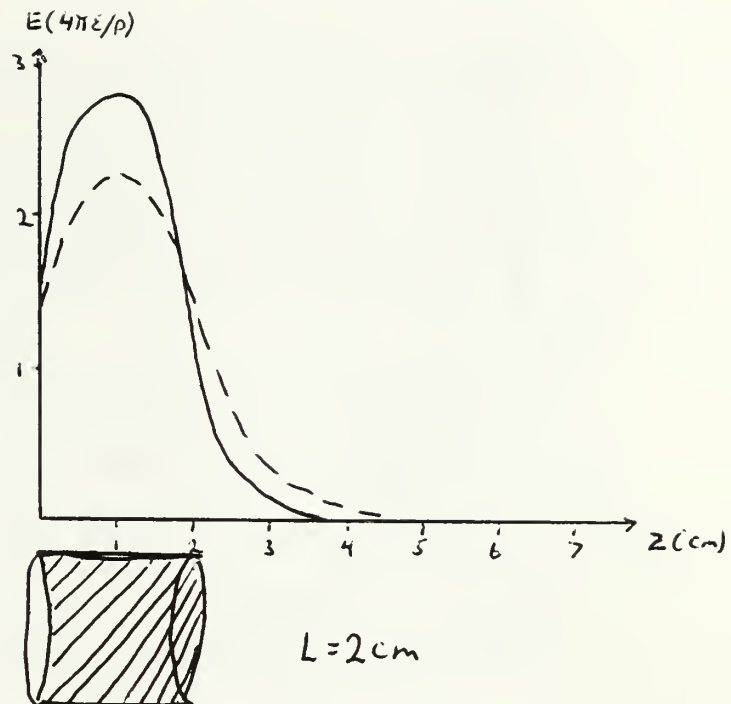
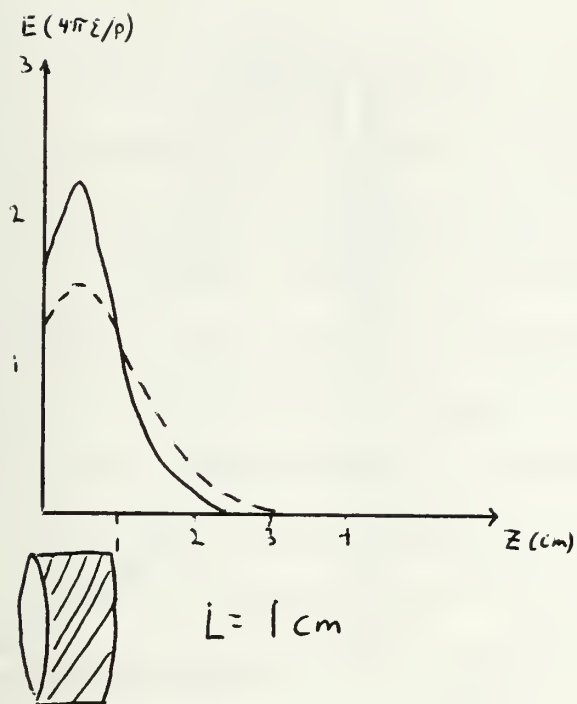
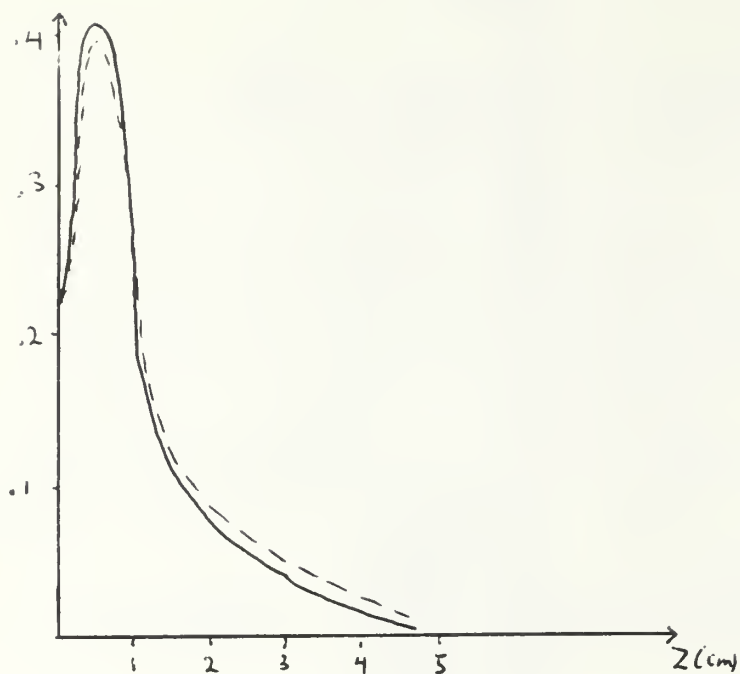
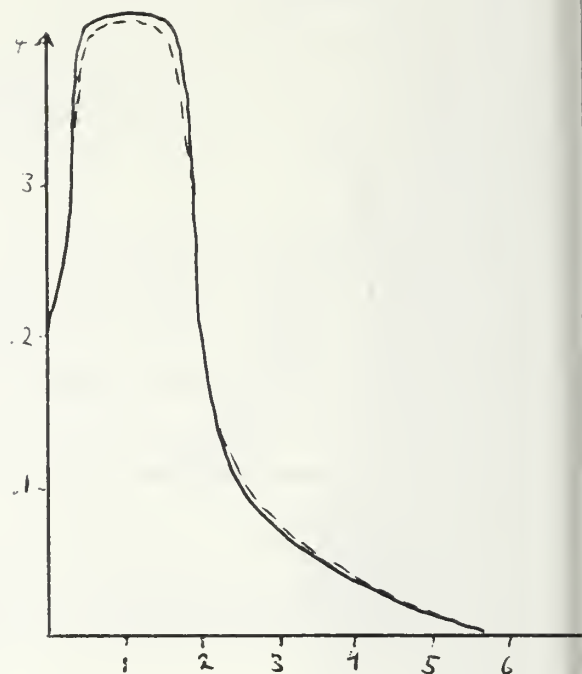


Figure 8:  $E(4\pi\epsilon/\rho)$  vs  $Z$  for cylinders of various lengths  
 $a_0 = 1 \text{ cm}$ ,  $b = .5 \text{ cm}$



$L = 1 \text{ cm}$



$L = 2 \text{ cm}$

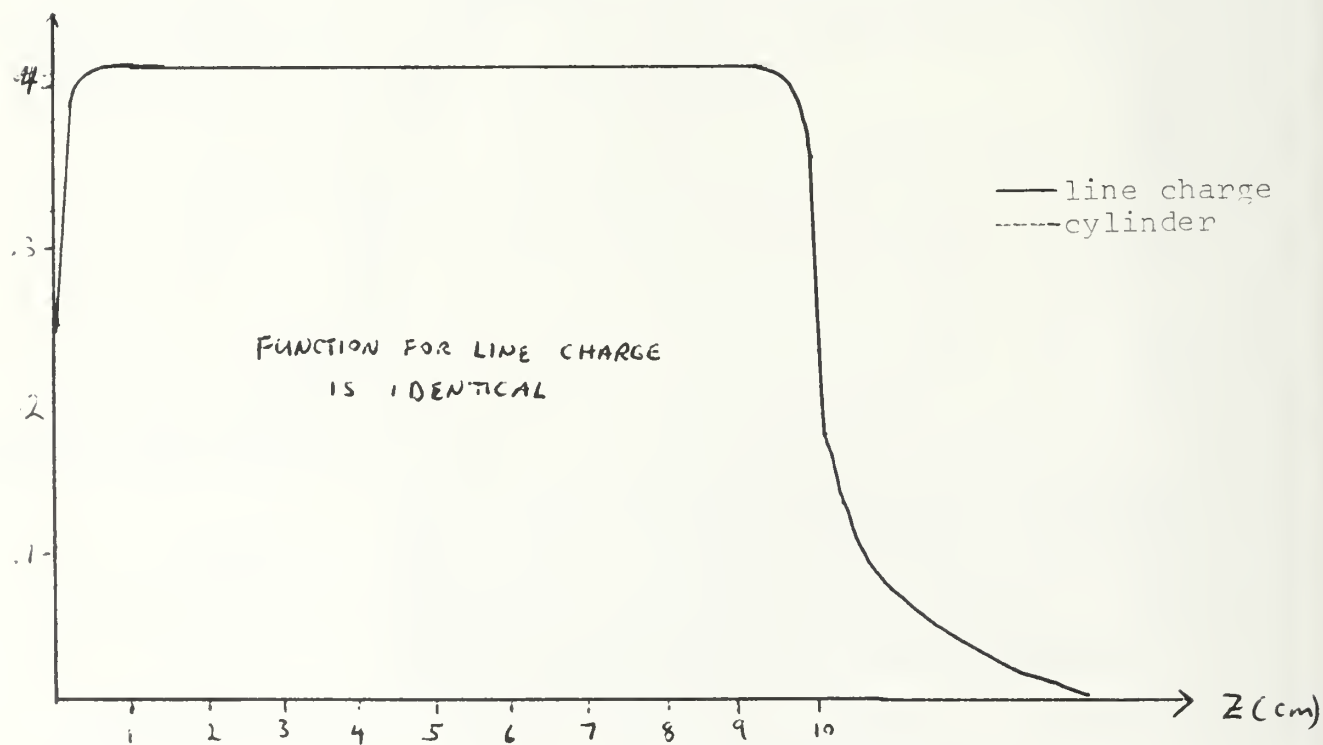


Figure 9:  $E (4\pi\epsilon_0/\rho)$  vs  $Z$  for cylinders of various lengths  
 $a_0 = .1 \text{ cm}$ ,  $b = .15 \text{ cm}$

fields. Even in this most extreme example, however, the approximation should be adequate for our purposes. As the bunch length increases, the actual and approximate fields are found to agree very closely with a slightly steeper rise in the linear approximation.

In conclusion, we find that treating the cylindrical charge distribution as a modified line charge offers a very satisfactory approximation to the actual fields present. Using this approximation for a static charge bunch, one can compute very closely the Fourier components of a relativistic charge bunch.

## APPENDIX B

### DIFFERENCES WITH THE THEORY OF TER-MIKAELIAN

In Chapter III, it was brought to the reader's attention that the equations derived in this paper were slightly at odds with the results presented by Ter-Mikaelian in Reference 1. In his paper, Ter-Mikaelian stated his results for an electron passing through the center of a circular aperture of radius  $a_0$  for  $\omega a_0 / v\gamma \ll 1$  (in Gaussian units).

$$E_x = \frac{ie}{2\pi^2 c} \frac{q}{q^2 + \alpha^2} J_0(qr_0) \cos \psi$$

$$E_y = \frac{ie}{2\pi^2 c} \frac{q}{q^2 + \alpha^2} J_0(qr_0) \sin \psi$$

where:

$$\alpha = \omega / v\gamma$$

$$q = k \sin \theta = \text{projection of the wave vector on the } z = 0 \text{ plane}$$

$$\psi = \text{the angle between } \vec{q} \text{ and the X-axis}$$

These equations give a radial field equal to

$$E_{\perp} = \frac{ie}{2\pi^2 c} \frac{q}{q^2 + \gamma^2} J_0(qr_0) .$$

Since this equation appears to be inconsistent with the equations derived in this paper, this appendix will explain



at length the method used to obtain the Bessel function in the equation.

The integral over  $d\theta$  in the Fraunhofer diffraction problem was written as

$$\int_0^{2\pi} \cos \theta e^{i(kbX/R) \cos \theta} d\theta \quad db .$$

The  $\cos \theta$  term in this integral is due to the radial nature of the electric field. Using the expression  $\cos \theta = (e^{i\theta} + e^{-i\theta})/2$ , the integral can be re-written as

$$\begin{aligned} & \int_0^{2\pi} \left( \frac{e^{i\theta} + e^{-i\theta}}{2} \right) e^{i(kbX/R) \cos \theta} d\theta \\ &= \frac{1}{2} \int_0^{2\pi} e^{i\left(\theta + \frac{kXb}{R} \cos \theta\right)} + e^{i\left(-\theta + \frac{kXb}{R} \cos \theta\right)} d\theta . \end{aligned}$$

Since  $J_m(u) = \frac{i^{-m}}{2\pi} \int_0^{2\pi} e^{i(mv + u \cos v)} dv$ , or

$$2\pi i^m J_m(u) = \int_0^{2\pi} e^{i(mv + u \cos v)} dv ,$$

the integral over  $d\theta$  is equivalent to

$$\pi i J_1(kXb/R) + \pi i^{-1} J_{-1}(kXb/R) = \pi i \left( J_1\left(\frac{kXb}{R}\right) - J_{-1}\left(\frac{kXb}{R}\right) \right) .$$

Since  $J'_n(x) = \{J_{n-1}(x) - J_{n+1}(x)\}/2$ , with  $n = 0$ , this expression reduces to

$$-2\pi i J'_0\left(\frac{kXb}{R}\right)$$

which equals

$$2\pi i J_1\left(\frac{kXb}{R}\right)$$

since  $J'_0(x) = -J_1(x)$ .

As shown earlier, the  $\sin \theta$  dependence of the diffraction pattern is given by

$$\frac{1}{q^2 + \alpha^2} [\kappa_0 \{qK_1(\alpha\kappa_0)J_2(q\kappa_0) - \alpha J_1(q\kappa_0)K_2(\alpha\kappa_0)\}] .$$

This appears to be quite different than that found by Ter-Mikaelian.

However, if one plots the two solutions, he will find they are identical.

## LIST OF REFERENCES

1. Ter-Mikaelian, M.L., High-Energy Electromagnetic Processes in Condensed Media, Wiley-Interscience, 1972.
2. Panofsky, W.K.H. and Phillips, M., Classical Electricity and Magnetism, Addison-Wesley, 1962.
3. Hecht, E. and Zajac, A., Optics, Addison-Wesley, 1974.
4. O'Grady, A., Cerenkov Radiation, Transition Radiation, and Diffraction Radiation from Periodic Bunches for a Finite Beam Path in Air, Master's Thesis, Naval Postgraduate School, Monterey, California, 1986.
5. Rule, D.W. and Fiorito, R.B., Naval Surface Weapons Center Technical Report Number NSWC TR 84-134, The Use of Transition Radiation as a Diagnostic for Intense Beams, July 1984.

## BIBLIOGRAPHY

Gröbner, W. and Hofreiter, N., Intergral tafel, Wien and Innsbruck, 1950.

Oberhettinger, F., Tabellen zur Fourier Transformation, Springer-Verlag, 1957.

Rule, D.W., Naval Surface Weapons Center Technical Report Number NSWC TR 86-180, Beam Targeting with Diffraction Radiation, April 1986.

Wheelon, A.D., Table of Summable Series and Integrals Involving Bessel Functions, Holden-Day, 1968.

INITIAL DISTRIBUTION LIST

	No. Copies
1. Defense Technical Information Center Cameron Station Alexandria, Virginia 22304-6145	2
2. Library, Code 0412 Naval Postgraduate School Monterey, California 93943-5000	2
3. Physics Library, Code 61 Department of Physics Naval Postgraduate School Monterey, California 93943-5000	2
4. Professor F.R. Buskirk, Code 61Bs Department of Physics Naval Postgraduate School Monterey, California 93943-5000	5
5. Professor J.R. Neighbours, Code 61Nb Department of Physics Naval Postgraduate School Monterey, California 93943-5000	5
6. Professor X.K. Maruyama B108, Bldg. 245 National Bureau of Standards Gaithersburg, Maryland 20899	2
7. Dr. Donald Rule, Code R41 Naval Surface Weapons Center White Oak Laboratory 10901 New Hampshire Avenue Silver Springs, Maryland 20903-5000	2
8. Dr. Ralph Fiorito, Code R41 Naval Surface Weapons Center White Oak Laboratory 10901 New Hampshire Avenue Silver Springs, Maryland 20903-5000	2
9. Dr. Joseph Mack M4, M.S. p-940 Los Alamos National Laboratory Los Alamos, New Mexico 87545	2



thesG14056

Diffraction radiation from relativistic



3 2768 000 75889 0

DUDLEY KNOX LIBRARY